

BIRZEIT UNIVERSITY  
FACULTY OF GRADUATE STUDY

Molecular Structure Optimization Energy and IR Calculations  
Of Photochemical Generated Chromium Metal Carbonyl using  
the Density Function Theory (DFT) Method

By

Zuhair-Shalalkeh

Submitted in Partial Fulfillment of the Requirement for the  
Master Degree in Scientific Computing From the Graduate  
Faculty at Birzeit University

Supervisor

Dr. Hani Awad  
Chemistry Department

Birzeit, Palestine  
Spring, 2005

Molecular Structure Optimization Energy and IR Calculations  
Of Photochemical Generated Chromium Metal Carbonyl using  
The Density Function Theory (DFT) Method

By

Zuhair-Shalaldeh

This thesis was successfully defended on June 16, 2005 and  
approved by:

Committee Members	Signature
1. Dr. Hani Awad	-----
2. Dr. Mazen Y. Hamed	-----
3. Dr. Wael Karain	-----
4. Dr. Omar Deeb	-----

## ABSTRACT

The Geometries, electronic structures and vibration frequencies of  $\text{Cr}(\text{CO})_6$ ,  $\text{Cr}(\text{CO})_5\text{pip}$ , were studied using the Hartree-Fock and B3LYP density functional level of theory combined with various basis sets. These methods have been implemented in the Gaussian 98 program. Comparison with experimental data shows that density functional theory with triple-split-valence polarized 6-311G (D) basis set gives good results for the structures and vibration frequencies of such compounds. The discrepancy between experimental and theoretical values results from the description of the wave function by a finite number of functions (basis sets). This introduces an approximation into the calculations since an infinite number of Gaussian functions would be needed to describe the wave function exactly. The same calculations have been performed on a series of carbonyl chromium complexes, of the type trans-(chlorobenzene)-(L) $\text{Cr}(\text{CO})_4$ , where L = CO,  $\text{PH}_3$ ,  $\text{PCl}_3$  and  $\text{PF}_3$ . The aim of this project is to explore the effect of these ligands on the Cr-Cl bond. The influences of the L ligands on the properties of these complexes are compared with the behavior of the carbonyl complex  $\text{Cr}(\text{CO})_6$ . The largest effect observed on the Cr-Cl bond is when L = CO. As the  $\pi$  back-bonding ability of the ligand Trans to chlorobenzene increases, the Cr-Cl bond distance increases. This effect in the octahedral complexes is similar to the Trans effect in square Planar complexes. The calculated IR frequencies in these

complexes are in good agreement with the reported experimental IR values.

## ملخص

لقد تمت دراسة الشكل و التركيبية الالكترونية وذبذبة الجزيئات لكل من المركبات التالية:

$\text{Cr}(\text{CO})_5\text{pip}$  و  $\text{Cr}(\text{CO})_6$  باستخدام الطرق المحوسبة (Hartree-Fock) باستخدام Basis sets مختلفة وذلك عن طريق برنامج Gaussian 98.

لقد أعطت Density Functional Theory نتائج جيدة بالنسبة للتركيبية الالكترونية والذبذبات الجزيئية مقارنة مع القيم المخبرية. و باستخدام نفس الطريقة تمت دراسة المركبات  $\text{trans}-(\text{CB})(\text{L})\text{Cr}(\text{CO})_4$  حيث ان:



الهدف من هذه الدراسة هو معرفة تأثير هذه ال Ligands على صفات هذه المركبات مقارنة مع  $\text{Cr}(\text{CO})_6$ . و في هذه الدراسة تبين ان تأثير  $\text{trans}$  CO على الرابطة Cr-CI كان هو الأكبر وهذا ناتج عن قدرة CO لتكوين  $\pi$ -back bonding.

أظهرت هذه الدراسة ان تأثير هذه ال Ligands في الشكل ذات الثمانية اوجه المنتظم (Octahedral) مشابه لنفس التأثير في المركبات التي تاخذ الشكل الرباعي المسطح (Square planar). كما واطهرت هذه الدراسة ان القيم المحوسبة لذبذبات الجزيئات في هذه المركبات مشابه للقيم المخبرية لذبذبات نفس الجزيئات.

## **Acknowledgments**

I would like to thank my academic supervisor Dr. Hani Awad for giving me the opportunity to work on this research project, encouraging me to work with electronic structure first-principles methods. His helping, collaboration and advice in all stages of this work were also appreciated. I am particularly thankful for the help and advice of Dr. Hijazi Abu Ali. Finally, I wish to thank my parents and my wife for their love and encouragement, without their help I would never have enjoyed so many opportunities.

# Contents

Abstract	II
Acknowledgments	IV
List of Figures	IX
List of Tables	XI
<b>1 Introduction</b>	<b>1</b>
<b>2 Overview of the Used Computational Methods</b>	<b>6</b>
2.1 Introduction	6
2.2 Quantum Mechanics	7
2.2.1 Schrödinger Equation	7
2.2.2 Schrödinger Equation for the Hydrogen Atom	8
2.2.3 The Schrödinger Equation for the Helium Atom Can not Be Solved Exactly	9
2.2.4 Perturbation Theory	11
2.2.5 Variation Method	12
2.2.6 Multi-Electron System	17
2.3 Basis Sets	19
2.3.1 Double Zeta Basis Sets	23
2.3.2 Split Valence Basis Sets	24
2.3.3 Triple Zeta Basis Sets	25
2.3.4 Notations	25
2.3.5 Polarized Basis Sets	28
2.3.6 Diffuse Functions	28

2.3.7 Basis Set Effects	29
2.4 Electronic Structure Calculations	29
2.4.1 Semi-Empirical Methods	30
2.4.2 Ab-initio Methods	30
2.4.3 The Hartree-Fock Approximation	30
2.4.4 The Limits of Hartree-Fock Method	33
2.4.5 The Density Functional Theory	34
<b>3 Software Packages and Computational Methodology</b>	<b>40</b>
3.1 Gaussian 98 Software	40
3.1.1 Running Gaussian 98	40
3.1.2 Using Gaussian Checkpoint	41
3.1.3 Checkpoint File Utilities	46
3.2 Chem3D	46
3.2.1 Viewing Gaussian Structures with Chem3D	47
3.3 Computational Details	48
3.4 Procedure	50
3.4.1 Single Point Calculations	50
3.4.2 Geometry Optimization	50
3.4.3 Optimization Algorithm	52
3.4.4 Frequency Calculations	53
<b>4 Reactivity and Bonding of Metal Carbonyl Complexes</b>	<b>55</b>
4.1 Introduction	55
4.2 Carbonyl Complexes	56

4.3 Phosphine Ligands	58
4.4 Trans-Effect (TE)	61
4.4.1 Introduction	61
4.4.2 Background	57
4.4.3 Structural Trans-effect (STE) In Octahedral Metal Complexes	63
4.4.5 Kinetic Trans-effect (KTE) in Octahedral Metal Complexes	63
<b>5 Results and Discussion</b>	<b>65</b>
5.1 Structure and Energy of Cr(CO) <sub>6</sub>	65
5.2 Predicted Geometry of Cr(CO) <sub>5</sub> pip	68
5.3 Vibrational Frequencies for Cr(CO) <sub>5</sub> pip	69
5.4 Structure and Properties of ( $\eta^1$ -chlorobenzene)Cr(CO) <sub>5</sub>	72
5.4.1 Carbonyl Frequencies of ( $\eta^1$ -chlorobenzene)Cr(CO) <sub>5</sub>	74
5.5 Structure and Properties of Trans-(CB)(L)Cr(CO) <sub>4</sub> Complexes, where L = CO, PH <sub>3</sub> , PCl <sub>3</sub> and PF <sub>3</sub>	78
5.6 Predicted Energy of trans-(CB)(L)Cr(CO) <sub>4</sub> Complexes, where L = CO, PH <sub>3</sub> , PCl <sub>3</sub> and PF <sub>3</sub>	82
5.7 Predicted Vibrational Frequencies of trans-(CB)(L)Cr(CO) <sub>4</sub> Complexes, where L = CO, PH <sub>3</sub> , PCl <sub>3</sub> and PF <sub>3</sub>	83
5.8 Potential Energy Surface Scans	86
5.8.1 Potential Energy Surface Scans of trans-(CB)(PCl <sub>3</sub> )Cr(CO) <sub>4</sub>	87
5.9 The Binding Energy	88

5.9.1 Overall Stability	89
<b>6 Conclusion</b>	<b>91</b>
References	93
7 Appendices	101
7.1 Atomic Units	101
7.2 Glossary	101
7.3 What's an "operator"?	104
7.4 Functional	104
7.5 Input Structure of Some Molecules Used in This Study	105

## List of Figures

1.1 Pulsed laser flash photolysis of cis-(pip)(L)Cr(CO) <sub>4</sub> in the presence of chlorobenzene (CB) leads to the formation of cis and trans-(CB)(L)Cr(CO) <sub>4</sub> (pip is piperidine and L = CO, PH <sub>3</sub> , PCl <sub>3</sub> or P(OCH <sub>3</sub> ))	3
2.1 A comparison of the normalized Slater orbital to the Gaussian orbital, with orbital exponents $\zeta = 1.24$ , and $\alpha = 0.4166$ , respectively	22
2.2 The Slater $\phi_{1s}^{STO}$ orbital is compared by sums of different numbers of Gaussian functions	23
3.1 Main program window	43
3.2 Job entry window	44
3.3 Molecular specification of Cr(CO) <sub>6</sub> in cartesian coordinate	44
3.4 Points on a potential energy surface	51
4.1 $\sigma$ Bonding, orbital overlap in M-CO bonding. Arrow shows direction of electron flow, ligand to metal $\sigma$ bonding	57
4.2 $\pi$ Back-bonding. Metal-to-ligand $\pi$ back-bonding	57
4.3 $\sigma$ donation of the phosphine lone pair to an empty orbital on the metal	58
4.4 Backdonation from a filled metal orbital to an empty d orbital on the phosphine ligand	59
5.1 Optimized Structure of Cr(CO) <sub>6</sub> at HF/6-311G(d), bond length given in Angstrom	66
5.2 Optimized structure of Cr(CO) <sub>6</sub> at DFT/6-311G(d), bond	

length given in Angstrom	67
5.3 Optimized structure of $\text{Cr}(\text{CO})_5\text{pip}$ using DFT with 6-311G(d)	68
5.4 Experimental data vs. B3LYP data with applied constant scaling factor	71
5.5 The optimized structure of the ( $\eta^1$ -chlorobenzene) $\text{Cr}(\text{CO})_5$ using DFT with 6-311G(D) basis set	72
5.6 Schematic representation of $\text{Cr}(\text{CO})_6$ and $\text{Cr}(\text{CO})_5\text{CB}$	74
5.7 Experimental data vs. B3LYP data with applied constant scaling factor	76
5.8 Infrared active modes of metal Carbonyls	77
5.9 Optimized structure of $\text{trans}-(\text{CB})(\text{PH}_3)\text{Cr}(\text{CO})_4$	85
5.10 Plot of the energies of $\text{trans}-(\text{CB})(\text{PCl}_3)\text{Cr}(\text{CO})_4$ at each point of the Cr-CB bond distance at DFT level of theory using 6-311G(D) basis set	88

## List of Tables

2.1 The coefficient and orbital exponents for the five Gaussian functions of the ground state carbon atom in 5-31G basis set. These values are determined by an optimal fit of a linear combination of five Gaussian functions to a Slater orbital with $\zeta = 5.67$	27
5.1 Theoretical predictions of total energies, and bond lengths of $\text{Cr}(\text{CO})_6$ at HF level of theory with various basis sets	65
5.2 Theoretical predictions of total energies, and bond length of $\text{Cr}(\text{CO})_6$ at DFT with various basis sets	66
5.3 Optimized structure of $\text{Cr}(\text{CO})_5\text{pip}$ and the corresponding energy parameter using DFT with different basis sets	68
5.4 Calculated frequencies of trans CO in $\text{Cr}(\text{CO})_5\text{pip}$ at B3LYP with 6-311G(D)	69
5.5 Unscaled frequencies, scaled frequencies, intensity, experimental frequencies of CO in $\text{Cr}(\text{CO})_5\text{pip}$	71
5.6 Theoretical predictions of the bond length of ( $\eta^1$ -chlorobenzene) $\text{Cr}(\text{CO})_5$ using DFT level of theory with 6-311G(D) basis sets	73
5.7 Raw carbonyl frequency of the ( $\eta^1$ -chlorobenzene) $\text{Cr}(\text{CO})_5$ calculated at DFT level of theory with 6-311G(D) basis set, with the corresponding IR intensity and the experimental data	78
5.8 Unscaled frequencies, scaled frequencies, IR intensity and experimental frequencies of ( $\eta^1$ -chlorobenzene) $\text{Cr}(\text{CO})_5$ using DFT level	

of theory with 6-311G(D) basis set	79
5.9 Optimized parameters (bond length) of trans-(CB)(L)Cr(CO) <sub>4</sub> where L = CO, PH <sub>3</sub> , PCl <sub>3</sub> and PF <sub>3</sub> using DFT with 6-311G(D) basis set	82
5.10 The Cr-PPh <sub>3</sub> bond lengths of trans-Cr(CO) <sub>4</sub> (L) from	84
5.11 Predicted energies of trans-(CB)(L)Cr(CO) <sub>4</sub> complexes, where L = CO, PH <sub>3</sub> , PCl <sub>3</sub> and PF <sub>3</sub>	84
5.12 Unscaled vs. scaled metal carbonyl frequencies of trans (CB)(L)Cr(CO) <sub>4</sub> where L = CO, PH <sub>3</sub> , PCl <sub>3</sub> and PF <sub>3</sub>	85
5.13 Binding energy of Cr-CB of trans-(CB)(L)Cr(CO) <sub>4</sub> , where L = CO, PH <sub>3</sub> , PCl <sub>3</sub> , and PF <sub>3</sub>	90
7.1 Input structure of (CB)Cr(CO) <sub>5</sub> in cartesian coordinates	105
7.2 Input structure of trans-(CB)(PH <sub>3</sub> )Cr(CO) <sub>4</sub> in Cartesian coordinates	106
7.3 Input structure of trans-(CB)(PCl <sub>3</sub> )Cr(CO) <sub>4</sub> in Cartesian coordinates	107

# Chapter 1

## Introduction

One of the most important goals of computational chemistry is to calculate from first principles the various physical and chemical quantities [1]. These calculations require a solution of the electronic structure of the system in question, which is based upon the principles of quantum mechanics. Such calculations are very computer-intensive [2]. However, because of advances in computer storage capacity and processor performance, electronic structure calculations have been rapidly evolving. It is now possible to solve relevant problems in an acceptable amount of time [2]. The density-functional theory (DFT) makes a huge step towards this goal by changing the problem of many interacting electrons to that of non-interacting particles under the influence of an effective potential [3].

Computational chemistry opens the door for chemists to simulate chemical structures and reactions numerically. These chemical phenomena are simulated rather than occurring experimentally [4]. Furthermore; computational chemistry can develop new materials, and can accelerate the research by reducing the cost and the risk to personnel testing of energetic materials [2], because handling a single compound could require months of labor and raw materials, and generate toxic waste [5].

Geometrical optimization and infrared (IR) calculations of transition metal complexes by the DFT method proved to be very successful and requires less CPU time. The use of the LanL2dz and the 6-311G (D) basis set with DFT for quantum chemical calculations of several inorganic molecules were shown to give satisfactory results when compared with experimental data [6].

Transition metal carbonyl systems are of great interest in many areas of chemistry, ranging from organometallic synthesis to catalysis [7]. The chemistry of the main group organometallic is governed by the metal in the compound, whereas for the transition group organometallic, the metal and the ligand nature dominate [8].

Pulsed laser flash photolysis of  $\text{cis}-(\text{pip})(\text{L})\text{Cr}(\text{CO})_4$  in the presence of chlorobenzene (CB) leads to the formation of  $\text{cis}$  and  $\text{trans}-(\text{CB})(\text{L})\text{Cr}(\text{CO})_4$  (pip is piperidine and  $\text{L} = \text{CO}, \text{PH}_3, \text{PCl}_3$  or  $\text{P}(\text{OCH}_3)$ ) as shown in Figure 1.1. Dobson and co-workers have shown that the CB replacement of the  $\text{cis}$  formed intermediate takes place at a faster rate than the  $\text{trans}$  intermediate [9]. The rate of CB displacement from the  $\text{cis}$  intermediate increases with the size of L bonded to the metal center [10]. Furthermore, the nature of bonding of CB with the metal center, in this case chromium was shown to take place between the chlorine and chromium [11]. Upon laser flash photolysis of  $\text{cis}-(\text{pip})(\text{L})\text{Cr}(\text{CO})_4$  the pip is lost and the vibration excited five coordinate intermediate will isomerizes to form the vacant  $\text{cis}$  site to L and the vacant  $\text{trans}$  site. The

solvent such as (CB) will occupy these vacant sites on a Pico-second time scale and it will be replaced by the incoming ligand on the micro to millisecond time scale. In these time scales, there is no evidence for thermally induced isomerization from cis to trans or vice-versa of five coordinate intermediate was seen to take place [10].

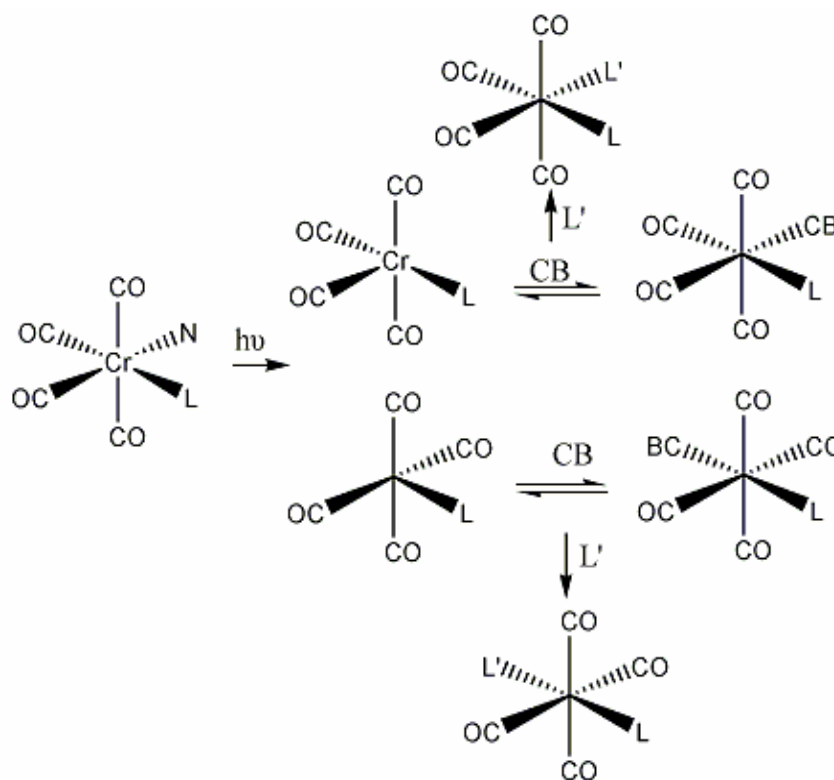


**Figure 1.1** Pulsed laser flash photolysis of cis (pip)(L)Cr(CO)<sub>4</sub> in the presence of chlorobenzene (CB) leads to the formation of cis and trans (CB)(L)Cr(CO)<sub>4</sub> (pip is piperidine and L = CO, PH<sub>3</sub>, PCl<sub>3</sub>, P(OCH<sub>3</sub>)) [10].

Since the last two decades, Scientists focused their attention on ligand substitution reactions of stable Group 6 metal carbonyls and their substitution products, (L)<sub>n</sub>M(CO)<sub>6-n</sub>. Similar complexes containing much more weakly coordinating ligands (L<sub>w</sub>, such as CB, which contains Cl as functional group, have been studied by flash photo-analysis [11,12]. This

research expanded these later studies through a detailed investigation of the displacement (CB), which coordinates to Cr through Cl. The study of the electronic effect of ligands on the metal environment was the center of attention in inorganic chemistry [10, 11, 12]. In octahedral chromium complexes, two positions for a selected ligand L, namely the cis and trans are possible. In this work the trans effect was discussed. As a starting point, the geometry of  $\text{Cr}(\text{CO})_6$  was optimized, using DFT and HF with various basis sets. The optimized structures reported here were obtained from gas phase calculations. The optimized bond lengths Cr-CO, C-O were compared with reported experimental values [4]. Results obtained by DFT using the 6-311G(D) basis set are in good agreement with the reported experimental values. Electronic structure calculations of  $\text{Cr}(\text{CO})_5\text{pip}$  have been performed. These calculations were based on the fully optimized geometries; frequency calculations were also performed, and compared with the reported experimental data. Structure and properties of  $\text{trans}-(\text{CB})(\text{L})\text{Cr}(\text{CO})_4$  where  $\text{L} = \text{CO}, \text{PCl}_3, \text{PF}_3, \text{PH}_3$  were carefully discussed in Chapter 5 to explore the effect of these ligands on the Cr-Cl bond.

In addition, binding energies of chromium complexes were also discussed. This should give us important information about the bonding properties of metal complexes.

The work presented in this thesis is based on density functional calculations, all of which have been carried out with the Gaussian 98

program. Density functional theory (DFT) is based on the two basic theorems by Kohn and Hohenberg which state that the ground state energy of the N-electron systems is a unique functional of the electron density distribution [13]. The theorems are quite important since they allow one to concentrate on the search for the electron density of the system, rather than the many-body quantum wave function, which is a much more complicated object. DFT, which used extensively in chemistry and physics, had great success in explaining and calculating the electronic structure of molecules and solids. DFT also provides information on the electron density distribution and ground state energy in a system of interest. There are many variants of DFT, possibly the most promising are those dealing with time dependent implementation of DFT. Walter Kohn and John A. Pople received a Nobel Prize in chemistry (1998) for the development of the density functional theory and related computational methods in quantum chemistry [13,14,15].

## **Chapter2**

### **Overview of the Used Computational Methods**

All work carried out in this study was based on quantum mechanics.

This chapter will introduce the most important theoretical concepts needed to understand how the results were obtained.

#### **2.1 Introduction**

Chemists used plastic models to help them understand and visualize the structures of molecules [5]. Recently both students and experienced researchers have begun to use chemical drawing programs for the same purpose [4]. Computational chemistry simulates chemical structures and reactions which are numerically based, in full or in part, on the fundamental laws of physics. It allows chemists to study chemical phenomena by running calculations on computers rather than by examining reactions and compounds experimentally [4]. Some methods can be used to model, not only stable molecules, but also short-lived unstable intermediates and transition states. In this way, they can provide information about molecules and reactions which is impossible to obtain through direct observation. Computational chemistry is, therefore, both an independent research area and a vital extra to experimental studies [2, 4, 5].

## 2.2 Quantum Mechanics

Quantum mechanics researchers are interested in understanding of how the electrons in molecules are behaving. Considering fundamental physics of electrons and atoms, quantum mechanics provides detailed information on these issues [4]. Quantum chemistry is concerned with the energy calculations of molecules and how this energy depends on structure. This subject is very important to chemists since the stability and the structure of the molecules depend on their energies [5].

### 2.2.1 Schrödinger Equation

Quantum mechanics states that the energy and other related properties of a molecule may be obtained by solving the Schrödinger equation [4]:

$$H\Psi = E\Psi \quad (2.1)$$

The Schrödinger equation is an eigenvalue problem. The operator on the left hand side of Equation 2.1 operates on the wave function that describes the wave-like nature of an electron. The wave function is represented by  $\psi$ . The result is the same wave function multiplied by constant. The operator from the left-hand side of Equation 2.1 is called a Hamiltonian operator which is symbolized by H [5]. When Equation 2.1 is solved, the result is a set of possible wave functions (called eigenfunctions)  $\psi_k$  and corresponding energies (eigenvalues)  $E_k$ . The eigenfunction  $\psi_0$  corresponds to the lowest energy  $E_0$ . It describes the ground

state of the system, and the higher energy values correspond to excited states.

### 2.2.2 Schrödinger Equation for the Hydrogen Atom

The Hydrogen atom is of particular interest to chemists because it serves as the prototype for more complex atoms and, therefore molecules. The hydrogen atom will be pictured as a proton fixed at the origin and an electron of mass  $m_e$  interacting with the proton through a Coulombic potential [16, 17]:

$$V(r) = \frac{e^2}{4\pi\epsilon_0 r} \quad (2.2)$$

Where  $e$  is the charge,  $\epsilon_0$  is the permittivity constant of the free space, and  $r$  is the distance between the electron and the proton. The spherical geometry of the model suggests that spherical coordinates is suitable to be used, with the proton at the origin. The Hamiltonian operator for the hydrogen atom is

$$\hat{H} = -\frac{\hbar^2}{2m_e} \nabla^2 - \frac{e^2}{4\pi\epsilon_0 r} \quad (2.3)$$

where  $\nabla$  is the Laplacian operator in spherical coordinates:

$$\nabla^2 = \frac{1}{r^2} \frac{\partial}{\partial r} \left( r^2 \frac{\partial}{\partial r} \right) + \frac{1}{r^2 \sin \theta} \frac{\partial}{\partial \theta} \left( \sin \theta \frac{\partial}{\partial \theta} \right) + \frac{1}{r^2 \sin^2 \theta} \frac{\partial^2}{\partial \phi^2} \quad (2.4)$$

If Equation 2.4 is substituted into Equation 2.3, the Schrödinger equation for the hydrogen atom becomes

$$-\frac{\hbar^2}{2m_e} \left[ \frac{1}{r^2} \frac{\partial}{\partial r} \left( r^2 \frac{\partial \Psi}{\partial r} \right) + \frac{1}{r^2 \sin \theta} \frac{\partial}{\partial \theta} \left( \sin \theta \frac{\partial^2 \Psi}{\partial \phi^2} \right) \right] - \frac{e^2}{4\pi\epsilon_0 r} \psi(r, \theta, \phi) \quad (2.5)$$

$$= E \psi(r, \theta, \phi)$$

Equation 2.5 can be solved exactly, giving a series of hydrogen-like atomic orbital wave functions of the form [17]

$$\Psi_{nlm}(r, \theta, \phi) = R_{nl}(r) Y_m(\theta, \phi) \quad (2.6)$$

where  $n, l, m$  are quantum numbers. For  $n = 1, l = 0, m = 0$ , it gives

$$\Psi_{1s} = \frac{1}{\sqrt{\pi}} \left( \frac{Z}{a_0} \right)^{\frac{3}{2}} e^{-\sigma} \quad (2.7)$$

and if  $n = 2, l = 1, m = 0$ , then

$$\Psi_{2p_z} = \frac{1}{\sqrt{32\pi}} \left( \frac{Z}{a_0} \right)^{\frac{3}{2}} \sigma e^{-\frac{\sigma}{2}} \cos \theta \quad (2.8)$$

The quantity  $Z$  is the atomic number of the nucleus and

$$\sigma = \frac{Zr}{a_0} \quad (2.9)$$

where  $a_0$  is the Bohr radius [15].

### 2.2.3 The Schrödinger Equation for the Helium Atom Cannot Be Solved Exactly

The Schrödinger equation for the helium atom is

$$\left( -\frac{\hbar^2}{2M} \nabla^2 - \frac{\hbar^2}{2m_e} \nabla_1^2 - \frac{\hbar^2}{2m_e} \nabla_2^2 \right) \Psi(R, r_1, r_2) + \left( -\frac{2e^2}{4\pi\epsilon_0 |R - r_1|} - \frac{2e^2}{4\pi\epsilon_0 |R - r_2|} + \frac{e^2}{4\pi\epsilon_0 |r_1 - r_2|} \right) \Psi = E \Psi(R, r_1, r_2) \quad (2.10)$$

In this equation,  $R$  is the position of the helium nucleus and  $r_1$  and  $r_2$  are the positions of the two electrons,  $M$  is the mass of the nucleus and  $\nabla_1^2$  and  $\nabla_2^2$  are the Laplacian operators with respect to the positions of the electronic coordinates. This is a three-body problem and not a two-body problem, so the separation into center of mass and relative coordinates is more complicated than for hydrogen atom [18]. However, because  $M \gg m_e$ , it is still an excellent approximation to regard the nucleus as fixed with no motion. This is known as the Born-Oppenheimer approximation [17]. Under this approximation, it is possible to fix the nucleus at the origin of a spherical coordinates system and write the Schrödinger equation as [15]:

$$-\frac{\hbar^2}{2m_e}(\nabla^2 + \nabla^2)\Psi(r_1, r_2) - \frac{2e^2}{4\pi\epsilon_0}\left(\frac{1}{r_1} + \frac{1}{r_2}\right)\Psi(r_1, r_2) + \frac{e^2}{4\pi\epsilon_0|r_1 - r_2|}\Psi(r_1, r_2) = E\Psi(r_1, r_2) \quad (2.11)$$

This simplified equation can not be solved exactly.

The term

$$\frac{e^2}{4\pi\epsilon_0|r_1 - r_2|} \quad (2.12)$$

causes difficulty. This term is called the interelectronic repulsion term and is directly responsible for the difficulty associated with solving Equation 2.11. Without it, the total Hamiltonian operators in Equation 2.11 would be the sum of the Hamiltonian operators of two hydrogen-like atoms, and the total energy would be the sum of the energies of the two individual

hydrogen-like atoms. Also the wave function would be a product of two hydrogen-like atomic orbitals. To solve Equation 2.11, approximation methods must be used. Two such methods have found wide use in quantum chemistry and yield extremely good results:

- ▣ Perturbation theory
- ▣ Variation method

#### 2.2.4 Perturbation Theory

The idea behind perturbation theory is as following: If it is impossible to solve the Schrödinger equation

$$\hat{H}E = E\Psi \quad (2.13)$$

for some system of interest, but it is not possible to solve it for another system that in some sense similar, then it is possible to write the Hamiltonian operator as

$$\hat{H} = \hat{H}^{(0)} + \hat{H}^{(1)} \quad (2.14)$$

Where

$$\hat{H}^{(0)}\Psi^{(0)} = E^{(0)}\Psi^{(0)} \quad (2.15)$$

This Schrödinger equation is possible to solve exactly [15]. The first term in Equation 2.14  $\hat{H}^{(0)}$  is called the unperturbed Hamiltonian operator and the additional term represents the perturbation. To apply perturbation

theory to the solution of Equation 2.13,  $\psi$  and  $E$  may be written in the form

$$\Psi = \Psi^{(0)} + \Psi^{(1)} + \Psi^{(2)} + \dots \quad (2.16)$$

and

$$E = E^{(0)} + E^{(1)} + E^{(2)} + \dots \quad (2.17)$$

where  $\psi^{(0)}$  and  $E^{(0)}$  are given by the solution to the unperturbed problem Equation 2.15 and  $\psi^{(1)}, \psi^{(2)}, \dots$  are successive corrections to  $\psi^{(0)}$  and  $E^{(1)}, E^{(2)}, \dots$  are successive corrections to  $E^{(0)}$ . Here the discussion will be limited to the first order perturbation theory, that is,  $H^{(1)}, \psi^{(1)}$ , and  $E^{(1)}$ .

$E^{(1)}$  is giving by

$$E^{(1)} = \int \Psi^{(0)} H^{(1)} \Psi^{(0)} d\tau \quad (2.18)$$

$E^{(1)}$  is the first order correction to  $E^{(0)}$  and

$$\Psi = \Psi^{(0)} + \Psi^{(1)} \quad (2.19)$$

$$E = E^{(0)} + E^{(1)} \quad (2.20)$$

Equation 2.20 represents the energy through first order perturbation theory [15].

### 2.2.5 Variation Method

While it is impossible to solve the Schrödinger equation exactly for multi-electron systems, one can get approximate solutions given enough

time to compute any desired accuracy. Considering the ground state of some particular arbitrary system, the ground state wave function  $\psi_0$  and energy  $E_0$  satisfy the Schrödinger equation

$$\hat{H}\Psi_0 = E_0 \Psi_0 \quad (2.21)$$

If the left hand side of Equation 2.21 is multiplied by  $\psi_0^*$ , and the resulting equation is integrated over all space, then the ground state energy can be written as:

$$E_0 = \frac{\int \Psi_0^* H \Psi_0 d\tau}{\int \Psi_0^* \Psi_0 d\tau} \quad (2.22)$$

A theorem says that if any other function  $\phi$  is substituted instead of  $\psi_0$  in Equation 2.22 and the corresponding energy calculated according to Equation

$$E_\phi = \frac{\int \phi^* H \phi d\tau}{\int \phi^* \phi d\tau} \quad (2.23)$$

then  $E_\phi$  will be greater than the ground-state energy  $E_0$ . [19]. The variation principle states that

$$E_\phi \geq E_0 \quad (2.24)$$

where the equality holds only if  $\phi = \psi_0$ . According to the variation principle, it's possible to calculate an upper bound to  $E_0$  by using any trial function. The closer  $\phi$  is to  $\psi_0$ , the closer  $E_\phi$  will be to  $E_0$ . It is possible

to choose a trial function  $\phi$  that depends upon some arbitrary parameters,  $\alpha, \beta, \gamma, \dots$ , called variation parameters. The energy also will depend upon these variation parameters, and Equation 2.24 becomes

$$E_{\phi}(\alpha, \beta, \gamma, \dots) \geq E_0 \quad (2.25)$$

It is possible to minimize  $E_{\phi}$  with respect to each of the variation parameters and determine the best possible ground-state energy which can be obtained from the trial wave function used. It is possible to use a trial wave function of the form

$$\phi = \sum_{n=1}^N c_n f_n \quad (2.26)$$

where the  $c_n$  are variation parameters and  $f_n$  are arbitrary known functions. For simplicity assume that  $N = 2$ , and that  $c_n$  and  $f_n$  are real.

With this simplification Equation 2.26 can be written as

$$\phi = c_1 f_1 + c_2 f_2 \quad (2.27)$$

Then, substituting into Equation 2.23 one will get

$$\begin{aligned} \int \phi \hat{H} \phi d\tau &= \int (c_1 f_1 + c_2 f_2) \hat{H} (c_1 f_1 + c_2 f_2) d\tau = \\ &= c_1^2 \int f_1 \hat{H} f_1 d\tau + c_1 c_2 \int f_1 \hat{H} f_2 d\tau + c_1 c_2 \int f_2 \hat{H} f_1 d\tau + c_2^2 \int f_2 \hat{H} f_2 d\tau \quad (2.28) \\ &= c_1^2 H_{11} + c_1 c_2 H_{12} + c_1 c_2 H_{21} + c_2^2 H_{22} \end{aligned}$$

where

$$H_{ij} = \int f_i \hat{H} f_j d\tau \quad (2.29)$$

a Hermitian operator must satisfy

$$\int f_i \hat{H} f_j d\tau = \int f_j \hat{H} f_i d\tau \quad (2.30)$$

Hence,

$$\int \phi \hat{H} \phi d\tau = c_1^2 H_{11} + 2c_1 c_2 H_{12} + c_2^2 H_{22} \quad (2.31)$$

and

$$\int \phi^2 d\tau = \int (c_1 f_1 + c_2 f_2)(c_1 f_1 + c_2 f_2) d\tau \quad (2.32)$$

this can be written as

$$\int \phi^2 d\tau = \int c_1^2 S_{11} + 2c_1 c_2 S_{12} + c_2^2 S_{22} \quad (2.33)$$

The quantities  $H_{ij}$  and  $S_{ij}$  are called matrix elements. By substituting Equations 2.30 and 2.32 into Equation 2.23, Equation 2.23 can be written as

$$E(c_1, c_2) = \frac{c_1^2 H_{11} + 2c_1 c_2 H_{12} + c_2^2 H_{22}}{c_1^2 S_{11} + 2c_1 c_2 S_{12} + c_2^2 S_{22}} \quad (2.34)$$

this can be written as

$$E(c_1, c_2)(c_1^2 S_{11} + 2c_1 c_2 S_{12} + c_2^2 S_{22}) = (c_1^2 H_{11} + 2c_1 c_2 H_{12} + c_2^2 H_{22}) \quad (2.35)$$

If Equation 2.35 is differentiated with respect to  $c_1$ ,

and letting

$$\frac{\partial E}{\partial c_1} = 0 \quad (2.36)$$

then,

$$c_1(H_{11} - ES_{11}) + c_2(H_{12} - ES_{12}) = 0 \quad (2.37)$$

Similarly, By differentiating  $E(c_1, c_2)$  with respect to

$c_2$ , the result is

$$c_1(H_{12} - ES_{12}) + c_2(H_{22} - ES_{22}) = 0 \quad (2.38)$$

Equations 2.37 and 2.38 constitute a pair of linear algebraic equations for  $c_1$  and  $c_2$ . There is a nontrivial solution that is not simply  $c_1 = c_2 = 0$ , if and only if the determinant of the coefficients vanishes, or if and only if

$$\begin{vmatrix} H_{11} - ES_{11} & H_{12} - ES_{12} \\ H_{12} - ES_{12} & H_{22} - ES_{22} \end{vmatrix} = 0 \quad (2.39)$$

This determinant is called a secular determinant. When this 2 X 2 determinant is expanded, a quadratic equation in  $E$  will be obtained, called the secular Equation. The quadratic secular equation gives two values for  $E$ ; the smaller one will be taken as the variation approximation for the ground-state energy [15].

If a linear combination of  $N$  functions is used in Equation 2.26 as a trial function, then the secular determinant will be of the form

$$\begin{vmatrix} H_{11} - ES_{11} & H_{12} - ES_{12} & \dots & H_{1N} - ES_{1N} \\ H_{12} - ES_{12} & H_{22} - ES_{22} & \dots & H_{2N} - ES_{2N} \\ \cdot & \cdot & \dots & \cdot \\ \cdot & \cdot & \dots & \cdot \\ H_{1N} - ES_{1N} & H_{2N} - ES_{2N} & \dots & H_{NN} - ES_{NN} \end{vmatrix} = 0 \quad (2.40)$$

The secular equation associated with this secular determinant is an  $N^{\text{th}}$ -degree polynomial in  $E$ . The smallest root of the  $N^{\text{th}}$ -order secular equation is an approximation to the ground state energy. The determination of the smallest root must be done numerically for the value of  $N$  larger than two. This is a standard numerical problem, which needs a computer program. Trial functions can be a linear combination of functions that also contain variation parameters of the form

$$\phi = \sum_{j=1}^N c_j f_j \quad (2.41)$$

Where the  $f_j$  themselves contain variation parameters. The minimization of  $E$  with respect to the  $c_j$  and  $\alpha_j$  is fairly complicated, involving  $2N$  parameters, and must be done numerically. Fortunately, a number of readily available algorithms can be used to do this [15, 17].

### 2.2.6 Multi-Electron System

For electrons moving in three dimensions in the presence of nuclei and other electrons, the Hamiltonian will have five terms comprising kinetic and potential energies:

- ▣ Kinetic energy of nuclei.
- ▣ Kinetic energy of Electrons.
- ▣ Potential energy: Nuclear-nuclear repulsion.
- ▣ Potential energy: Nuclear-electron attraction.
- ▣ Potential energy: Electron-electron repulsion.

The full Hamiltonian for the molecular system can be written as [15, 19]:

$$\hat{H}_{tot} = \hat{T}_n + \hat{T}_e + \hat{U}_{nn} + \hat{U}_{en} + \hat{U}_{ee} \quad (2.42)$$

$\hat{T}_n$  is the operator of kinetic energy of nuclei

$\hat{T}_e$  represent the kinetic energy of the electrons

$\hat{U}_{nn}$  is the interaction energy of nuclei (Columbic repulsion)

$\hat{U}_{en}$  is the external potential (in this case, the electrostatic potential coming from nuclei with which the electron interacts)

$\hat{U}_{ee}$  denotes electrostatic repulsion between electrons [20].

and

$$\nabla^2 = \frac{\partial^2}{\partial x^2} + \frac{\partial^2}{\partial y^2} + \frac{\partial^2}{\partial z^2} \quad (2.43)$$

Using the Born-Oppenheimer simplification, it is possible to neglect the kinetic energy term of the nuclei, and the electronic Hamiltonian can be written as

$$\hat{H}^{elec} = -\sum_{i=1}^N \frac{1}{2} \nabla_i^2 - \sum_i \sum_A \frac{Z_A}{r_{iA}} + \sum_i \sum_{j>i} \frac{1}{r_{ij}} + \sum_A \sum_{B>A} \frac{Z_A Z_B}{|R_A - R_B|} \quad (2.44)$$

This Hamiltonian is then used in the Schrödinger equation describing the motion of electrons in the field of fixed nuclei [4, 15]:

$$H^{elec} \Psi^{elec}(r, R) = E^{eff}(R) \Psi^{elec}(r, R) \quad (2.45)$$

Solving this equation, the effective nuclear potential function  $E^{eff}$  is obtained, which will then be used in the nuclear Hamiltonian

$$H^{nucl} = T^{nucl}(R) + E^{eff}(R) \quad (2.46)$$

This Hamiltonian is then used in the Schrödinger equation for nuclear motion which is useful in predicting the vibration spectra of the molecules [4].

### 2.3 Basis Sets

The essential idea in quantum chemical calculations is that molecular orbitals are expanded as linear combinations of atomic orbitals which are known as basis set [15, 18, 19]

$$\Psi_i = \sum_{\mu}^n c_{i\mu} \phi_{i\mu} \quad (2.47)$$

where  $\Psi_i$  is the  $i^{\text{th}}$  molecular orbital,  $c_{i\mu}$  are the coefficients of linear combinations,  $\phi_{i\mu}$  is the  $\mu^{\text{th}}$  atomic orbital, and  $n$  is the number of atomic orbital. An orbital is the wave function of an electron which moves under the influence of the nuclear attraction and the average repulsion of all other electrons [5]. A basis set is a set of mathematical functions which describes the shape of the orbitals in an atom [5, 15]. These basis sets were combined to approximate the total electronic wave function which will be used in the calculation. Larger basis sets approximate the orbital more accurately because they impose fewer restrictions on the location of electrons in space [4, 21].

Basis sets were first developed by J.C. Slater which has the general form

$$\text{Basis function} = Ne^{(-\alpha r)} \quad (2.48)$$

where:

$N$  = normalization constant

$\alpha$  = orbital exponent

$r$  = radius in angstroms

These functions were used because of their similarity to the atomic orbital of hydrogen atom and they are known as Slater type orbitals (STO's) [18].

They can be described in spherical coordinates as

$$S_{nlm}(r, \theta, \phi) = Nr^{n-1}e^{-\xi r}Y_{lm}(\theta, \phi) \quad (2.49)$$

where  $N$  is a normalization constant,  $\zeta$  is called exponent,  $r$ ,  $\theta$ ,  $\phi$ , are spherical coordinates,  $Y_{lm}$  is the orbital angular momentum and  $n$ ,  $l$ ,  $m$  are the principle, angular momentum, magnetic quantum numbers, respectively [21]. Unfortunately, STO are not suitable for fast calculations because the integrals resulting from the secular determinants are difficult to evaluate [15, 19]. Therefore, Gaussian type orbitals (GTOs) were introduced. Gaussian and other ab-initio electronic structure programs use GTO as basis function [4, 15], which have the general form:

$$G(\alpha, \theta, \phi) = Nr^{n-1} e^{-\alpha r^2} Y_{lm}(\theta, \phi) \quad (2.50)$$

where:

$N$  = normalization constant

$\alpha$  = orbital exponent [4].

The Slater orbitals and the Gaussian orbitals behave differently for small values of  $r$  [15, 21]. Figure 2.1 compares a normalized  $S_{100} = \phi_{1s}^{STO}$  Slater orbital Equation (2.49) with a normalized  $G_{100} = \phi_{1s}^{GTO}$  (Equation 2.50) for a hydrogen atom, with orbital exponents  $\zeta = 1.24$  and  $\phi = 0.4166$  in  $\phi_{1s}^{STO}$  and  $\phi_{1s}^{GF}$ , respectively. In carrying out a calculation, we use

$$\phi_{1s}(r) = \phi_{1s}^{STO}(r, 1.24) \quad (2.51)$$

or

$$\phi_{1s} = \phi_{1s}^{GF}(r, 0.1466) \quad (2.52)$$

Depending on whether the Slater orbitals (STO) or Gaussian functions (GF) is used as a basis set, the 1s orbital in each of these basis sets is

$$\phi_{1s}^{STO} = \left(\frac{\zeta^3}{\pi}\right)^{\frac{1}{2}} e^{-\zeta r} \quad (2.53)$$

and

$$\phi_{1s}^{GF} = \left(\frac{2\alpha}{\pi}\right)^{\frac{3}{4}} e^{-\alpha r^2} \quad (2.54)$$

Figure 2.1 shows that the Slater orbital has a cusp at  $r = 0$ , whereas the slope of the Gaussian orbital is zero at  $r = 0$ . The Gaussian orbital does a reasonably good job of describing the Slater orbital for values of  $r$  greater than  $a_0$ . To overcome this difficulty, a number of researchers in quantum chemistry have fitted Slater orbitals to sums of Gaussian functions. The fit improved with  $N$ , where  $N$  is the number of Gaussian functions used.

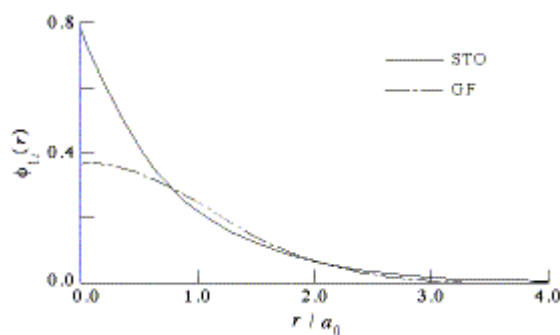


**Figure 2.1** A comparison of the normalized Slater orbital to the Gaussian orbital, with orbital exponents  $\zeta = 1.24$ , and  $\alpha = 0.4166$ , [15]

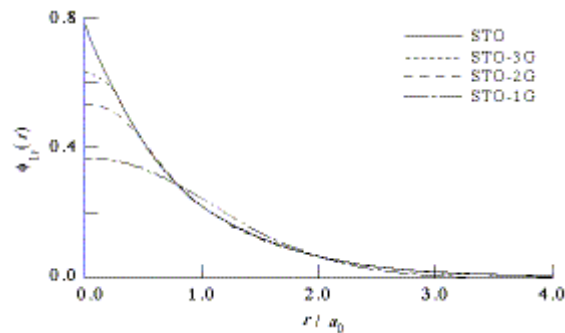


Figure 2.2 The Slater  $\phi_{1s}^{STO}$  orbital is compared by sums of different numbers of Gaussian functions [15]

Figure 2.2 shows this fit as a function of  $N$ . For example, for  $N = 3$ , the Slater orbital  $\phi_{1s}^{STO}(r, 1.24) = 0.779e^{-1.24r}$  is expressed by

$$\begin{aligned} \phi_{1s}^{STO}(r) &= \sum_{i=1}^3 d_{1si} \phi_{1s}^{GF}(r, \alpha_{1si}) = 0.4446 \phi_{1s}^{GF}(r, 0.1688) \\ &+ 0.5353 \phi_{1s}^{GF}(r, 0.6239) + \phi_{1s}^{GF}(r, 3.425) \end{aligned} \quad (2.55)$$

Because a sum of three Gaussian functions are used to represent one Slater orbital, such a basis set is called the STO-3G basis set. The general form of such basis sets is STO-NG ( $N = 1, 2, 3, \dots$ ) [4, 15].

### 2.3.1 Double Zeta Basis Sets

STO-NG ( $N = 1, 2, 3, \dots$ ) basis sets which uses finite sum of Gaussian functions to describe the atomic orbital results in several inadequacies that affect the accuracy of the calculations. Because the atomic orbitals in the STO-3G use fixed exponents,  $\alpha_{ki}$  or orbitals of a given type are identical in size. For example, the px, py, pz atomic orbitals all have the same radial function,  $re^{-\alpha r^2}$  (Equation 2.50), and thus are identical, but this will not

give an accurate picture of the electron density for a particular atom within the molecule. Computational chemists have solved this problem by expressing each atomic orbital as a sum of two Slater-type orbitals that differ only in the value of their exponents  $\zeta$ . The zeta value accounts for how diffuse the orbital is. For example, the 2s orbital is written as

$$\phi_{2s}(r) = \phi_{2s}^{STO}(r, \zeta_1) + d\phi_{2s}^{STO}(r, \zeta_2) \quad (2.56)$$

The Slater orbitals  $\phi_{2s}^{STO}(r, \zeta_1)$  and  $\phi_{2s}^{STO}(r, \zeta_2)$  represent different size 2s orbital. A linear combination of these two functions construct an atomic orbital whose size can range between that specified by  $\phi_{2s}^{STO}(r, \zeta_1)$  and  $\phi_{2s}^{STO}(r, \zeta_2)$  by varying the constant d. Such basis sets are called double-zeta basis sets because each orbital in the basis set is the sum of two Slater orbitals that differ only in their value of the orbital exponents,  $\zeta$  (zeta).

### 2.3.2 Split Valence Basis Sets

In general, only the valence orbitals are expressed by a double zeta representation. The inner-shell electrons are still described by a single Slater orbital. For example, the electrons in the 1s atomic orbital on a carbon atom would be described by a single  $\phi_{1s}^{STO}$  Slater orbital, where as the electrons in the 2s atomic orbital would be described by a linear combination of two  $\phi_{2s}^{STO}$  Slater orbitals with different values of the orbital exponents,  $\zeta$ . Such basis sets are referred to as split-valence basis sets. To facilitate the evaluation of the secular determinant, each Slater orbital in

the split valence basis set is expressed in terms of Gaussian functions. Thus, each of the two Slater orbitals,  $\phi_{2s}^{STO}(r, \zeta_1)$  and  $\phi_{2s}^{STO}(r, \zeta_2)$ , in Equation 2.56 is a linear combination of Gaussian functions. In principle, any number of Gaussian functions can be used to describe  $\phi_{1s}^{STO}$  and  $\phi_{2s}^{STO}$  [15].

### 2.3.3 Triple Zeta Basis Sets

Triple zeta basis set consists of three Slater orbitals with different values of zeta to fit one of the orbitals. The common triple basis set used is 6-311G, where six tells us that the inner shell orbital is represented by a linear combination of six Gaussian functions. The 311 tells us that the valence orbitals are represented by triple zeta basis sets. In other words, every valence orbital is represented by three Slater orbitals. The smaller Slater orbital is represented by three Gaussian functions, and the other two Slater orbital are each represented by one Gaussian function [4, 5].

### 2.3.4 Notations

The notations used to tell us the number of Gaussian functions used to describe the various Slater orbitals in a split valence basis set is N-MPG, where N is the number of Gaussian functions used to describe the inner-shell orbitals, the hyphen indicates that this is a split valence basis sets and M and P designate the number of Gaussian functions that are used to fit  $\phi_{1s}^{STO}$  and  $\phi_{2s}^{STO}$ , respectively. Because  $\zeta_1 > \zeta_2$  (by convention), M corresponds to the number of Gaussian functions used to express the

smaller Slater orbital and P corresponds to the number of Gaussian functions used to express the larger Slater orbital. The G simply tells that Gaussian functions are used. These basis sets are commonly referred to as Pople basis sets. For example, one popular basis set used extensively in computational chemistry is the 5-31G basis set. For carbon atom in a 5-31G basis set, the 5 tells us that the 1s orbital on the carbon atom (the inner-shell orbital) is given by a sum of 5 Gaussian functions. The hyphen indicates a split-valence basis set, telling us that the valence 2s and 2p orbitals are each represented by a pair of Slater orbitals. One of these Slater orbitals, the smaller one, is represented by a sum of three Gaussian functions (hence the 3), and the larger orbital is represented by a single Gaussian function, (hence the 1). Other Pople basis sets are 3-21G, 4-31G, 4-22G, 6-21G, 6-311G, and 7-41G. The time required to evaluate the elements of the secular determinant depends upon the number of functions used. One of the most important decisions in performing any calculation is the choice of the basis set. The label 5-31G indicates that the Gaussian basis set for which the inner-shell (1s) orbitals described by a sum of 5 Gaussian functions and the valence orbitals are described by a double-zeta representation where one Slater orbital (the smaller one) is represented by a linear combination of three Gaussian functions and the other Slater orbital (the larger one) is represented by a single Gaussian function. The 1s orbital in the 5-31G basis set is given by the best fit of a sum of 5 Gaussian functions to a single  $\phi_{1s}^{STO}$  Slater orbital using  $\zeta = 5.67$ . Thus,

$$\phi_{1s}^{STO} = \sum_{i=1}^5 d_{1si} \phi_{1si}^{GF}(r, \alpha_{1si}) \quad (2.57)$$

where the values for  $d_{1si}$  and  $\alpha_{1si}$  for the carbon atom in the 5-31G basis set are given in Table 2.1 [15].

Table 2.1 The Coefficient and orbital exponents for the five Gaussian functions of the ground state carbon atom in 5-31G basis set. These values are determined by an optimal fit of a linear combination of five Gaussian functions to a Slater orbital with  $\zeta = 5.67$

$\alpha_{1si}$	$d_{1si}$	$\alpha_{2si} = \alpha_{2pi}$	$d_{2si}$	$\alpha_{2s}$
1.264250	5.473496	7.942731	-1.207731	1.585120
1.901443	4.079115	1.907238	-1.697932	
4.312859	1.812203	5.535774	1.149812	
1.194438	4.634825			
3.651485	4.524712			

The 2s orbital is described by a double zeta basis set, or a linear combination of two  $\phi_{2s}^{STO}$  Slater orbitals,  $\phi_{1s}^{STO}(r, \zeta_1)$ ,  $\phi_{2s}^{STO}(r, \zeta_2)$  and of different orbital exponents,  $\zeta_1 > \zeta_2$ . The smaller Slater orbital,  $\phi_{1s}^{STO}(r, \zeta_1)$  is described by a linear combination of 3 Gaussian functions,  $\phi_{2s}^{STO}(r, \zeta_2)$  is described by a single Gaussian function. Thus,

$$\phi_{2s}^{STO}(r, \zeta_1) = \sum_{i=1}^5 d_{2si} \phi_{2s}^{GF}(r, \alpha_{2si}) \quad (2.58)$$

$$\phi_{2s}^{STO}(r, \zeta_2) = \phi_{2s}^{GF}(r, \alpha'_{2si}) \quad (2.59)$$

So the 2s orbital in 5-31G basis set is given by

$$\phi_{2s}(r) = \sum_{i=3}^3 d_{2si} \phi_{2s}^{GF}(r, \alpha_{2si}) + d'_{2s} \phi_{2s}^{GF}(r, \alpha'_{2si}) \quad (2.60)$$

### 2.3.5 Polarized Basis Sets

Split valence basis sets allow orbitals to change size, but not to change shape [4]. Functions which are responsible for changing the shape are called polarization functions. They have higher angular momentum than the occupied orbitals. Polarized basis sets change the shape of the orbital by adding, for example, d functions to carbon atoms and f functions to transition metals. Some of them add p functions to a hydrogen atom. For example: 6-31G (d), 6-31G (d,p). The latter polarized basis set adds a p function to hydrogen atom, and d function to heavy atoms, and some scientists refer to them as 6-31G\*, 6-31G\*\*, respectively [5]. Many basis sets are just identified by the author's surname and the number of primitive functions. Some examples of this are the Huzinaga, Dunning, and Duijneveldt basis sets. For example, D95 and D95V are basis sets created by Dunning with nine s primitives and five p primitives. The V implies one particular contraction scheme for the valence orbitals [5].

### 2.3.6 Diffuse Functions

For molecules which have electrons far from the nucleus: molecules with lone pairs, anions and other systems with significant negative charge,

diffuse function are used. The notation for the diffuse functions is as follow: single plus means that a diffuse function is added to heavy atoms such as 6-31+G(D), 6-31++G(D) adds diffuse function to hydrogen atom as well [22,23].

### **2.3.7 Basis Set Effects**

A basis set is the mathematical description of the orbitals within a system (where the total electronic wave function is approximated by combination of these basis sets) [4]. Since electrons have a finite probability of existing anywhere in space, larger basis sets approximate the orbital more accurately by imposing fewer restrictions on the locations of the electrons in space (bigger is always slower and usually more accurate) [4, 22]. Any difference in results due to the quality of one basis set versus another are referred as basis set effects [23].

## **2.4 Electronic Structure Calculations**

Electronic structure methods are based on the laws of quantum mechanics rather than classical physics [4]. This is, because the basis of electronic structure methods is the assumption that all chemistry can be described in terms of the interactions between electronic charges within the molecules [2]. There are two major classes of electronic structure methods:

### 2.4.1 Semi-Empirical Methods

Semi-empirical methods use parameters derived from experimental data to simplify the computations [4]. Several semi-empirical methods [2] are available and appear in commercially available computational chemistry software packages such as HyperChem and Chem3D [24].

### 2.4.2 Ab-initio Methods

The term ab-initio is given to computations that are derived directly from a theoretical principal with no inclusion from experimental data [5]. The term ab-initio implies that the computations are based solely on the laws of quantum mechanics, so it depends on masses and charges of electrons and atomic nuclei, the values of fundamental physical constants such as the speed of light ( $c = 2.998 \times 10^8$  m/s) or Planck's constant ( $h = 6.626 \times 10^{-34}$  J·s) and contain no approximations [2]. This is an approximate quantum mechanical calculation [15]. The approximation here means that they use mathematical approximations such as how to find approximate solutions for a differential equation [1]. Ab-initio molecular orbital computations can provide accurate quantitative predictions of chemical properties for a wide range of molecular systems. However, they place a considerable demand on computer resources [2].

### 2.4.3 The Hartree-Fock Approximation

One of the most popular Ab-initio methods used in electronic structure calculations is the Hartree-Fock method (abbreviated HF) [15]. In this

method, the electron-electron repulsion term is taken into account [19]. HF is useful in that it breaks the many-electron Schrödinger equation into many simpler one-electron equations [5]. In other words, the many electrons wave function  $\Psi$  is written as a product of one-electron function  $\phi$  for each of the N electrons [2, 25, 26]:

$$\Psi(r_1, r_2, \dots, r_N) = \phi_1(r_1)\phi_2(r_2)\dots\phi_N(r_N) \quad (2.61)$$

Which is known as a Hartree product [26].

Since the electronic Schrödinger equation

$$H^{elec}\Psi^{elec}(r, R) = E^{eff}(R)\Psi^{elec}(r, R) \quad (2.62)$$

Presents a multi-particle problem, approximations have to be considered for its solution. In the Hartree-Fock theory, the N particle wave function  $\Psi$  is described as an anti-symmetric product of N single particle functions  $\phi_i(r_i)$ , the so called Slater determinant [27]:

$$\Psi(r_1, r_2, \dots, r_N) = \frac{1}{\sqrt{N!}} \begin{vmatrix} \phi_1(r_1) & \phi_2(r_1) & \dots & \phi_N(r_1) \\ \phi_1(r_2) & \phi_2(r_2) & \dots & \phi_N(r_2) \\ \phi_1(r_3) & \phi_2(r_3) & \dots & \phi_N(r_3) \\ \dots & \dots & \dots & \dots \\ \phi_1(r_N) & \phi_2(r_N) & \dots & \phi_N(r_N) \end{vmatrix} \quad (2.63)$$

Here each electron is described by a spin orbital  $\phi_i(r_i)$  which is a product of a spatial orbital  $\Psi_i(x_i)$  that depends on the position of the electron  $x_i$  and a spin orbital  $\alpha(\omega)$  or  $\beta(\omega)$  that depends only on its spin

coordinates. Assuming the spin-orbital  $\phi_i(r_i)$  form a complete orthonormal basis, they are determined by variation methods, i.e. the expectation value of the Slater determinant with the electronic Hamiltonian operator becomes a minimum [27]:

$$E_{el} = \frac{\int \psi_{el}^* \hat{H}_{el} \psi_{el} d\tau}{\int \psi_{el}^* \psi_{el} d\tau} \quad (2.64)$$

This leads to the Hartree-Fock (HF) equations which give solutions to the orbital eigenenergies  $\varepsilon_i$  and the spin-orbitals  $\phi_i(r_i)$  for each electron  $i$  [28]

$$\hat{F}\phi_i(r_i) = \varepsilon_i \phi_i(r_i) \quad i = 1, \dots, N \quad (2.65)$$

The Fock operator  $\hat{F}$ ,

$$\hat{F}(r_i) = \hat{h}(r_i) + \hat{V}^{HF} = \hat{h}(r_i) + \sum_{j=1}^N [\hat{J}_j(r_i) - \hat{K}_j(r_i)] \quad (2.66)$$

Consists of the single particle operator

$$\hat{h}(r_i) = \frac{p_i^2}{2m_e} - \sum_{n=1}^{N_{nuc}} \frac{Z_n e}{|r_i - R_n|} \quad (2.67)$$

This describes the motion of a single electron in the field of the nuclear frame, and the Hartree-Fock potential which describes the interaction of each electron with all other electrons.  $\hat{V}^{HF}$  is composed of the Coulomb operator  $\hat{J}_j$

$$\hat{J}_j \phi_i(r_i) = \left[ \int dr_j \phi_j^*(r_j) \frac{1}{|r_i - r_j|} \phi_i(r_i) \right] \phi_i(r_i) \quad (2.68)$$

And the exchange operator  $\hat{K}_j$

$$\hat{K}_j \phi_i(r_i) = \left[ \int dr_j \phi_j^*(r_j) \frac{1}{|r_i - r_j|} \phi_i(r_i) \right] \phi_j(r_j) \quad (2.69)$$

The first term of  $\hat{V}^{HF}$  specifies an electron in the average field created by all other electrons. The second term arises from the anti-symmetric character of the Slater determinant in Equation 2.63. Since the Fock operator acting on the spin-orbitals  $\phi_i(r_i)$  depends itself on these functions via the Hartree-Fock potential  $\hat{V}^{HF}$ , an iterative method has to be used in order to solve the Hartree-Fock Equations 2.65. First, an initial guess of the spin-orbitals  $\phi_i$  is used to calculate  $\hat{J}$  and  $\hat{K}$  and, hence, the Fock operator  $\hat{F}$ . Then, the Hartree-Fock equations are solved yielding new  $\phi_i$  which are again used to calculate a new Fock operator. This procedure, known as the self consistent field method, is repeated until convergence is reached [1, 15, 19].

#### 2.4.4 The Limits of Hartree-Fock Method

Hartree-Fock theory is very useful for first level predictions of many systems. This is especially true for computing the structure and vibration frequencies of stable molecules and some transition states. However, it is

unsuitable for predicting accurate modeling of the reactions energy and bond dissociation because it is neglecting electron correlation [4, 15].

#### **2.4.5 The Density Functional Theory**

The development of the DFT method brought chemical accuracy at the beginning of the 1990's [29]. The progress in computer technology has made the DFT method the most powerful tool for the study of clusters, organometallics, and coordination chemistry.

The importance of the density functional theory is emphasized by the fact that W. Kohn, one of the DFT creators, received the Noble prize in chemistry in 1998. He shared it with J.A Pople [30]. In a first principles approach, the molecules are considered as a collection of atomic nuclei and a number of electrons. The electronic structure of these molecules is obtained by solving the Schrödinger equation for the many-particle wave function of the electrons. All other properties of atoms and molecules can then be determined [31]. However, these approaches have serious limitations:

- The resulting wave functions are complicated objects.
- As the number of interacting objects increases, the computational effort rapidly increases, and for larger systems this approach becomes prohibitive [32].

An alternative approach to conventional ab-initio methods in quantum chemistry which has emerged in recent years is the Density functional method (DFT) [31, 32, 33]. Instead of the many body wave function, the one body density is used as fundamental variable [29, 31, 34, 35, 36], which is a function of only three spatial coordinates rather than  $3N$  coordinates of the wave function. This makes density functional theory more feasible for large systems [37, 38]. The basic idea of the density functional theory is that the total ground state energy of an electron system can be written as a functional of the electron probability density  $\rho = \rho(r)$  [39, 40]. The electronic energy is said to be a functional of  $\rho$ , [36], which means that for a given density function  $\rho(r)$  there is only one energy value. The idea that electron density, and not the wave function, is the important quantity dates back to the 1920's with the Thomas-Fermi model (also known as the  $X\alpha$  model). The developments gained steam in the mid 60's with the arrival of a couple of articles of Walter Kohn and coworkers. In the first paper, Hohenberg and Kohn proved that the ground state energy (and all other ground state properties) of any system can be written as a function of electronic density. This provided the basis for modern Density Functional methods [13]. Unfortunately, the form of the functional dependence of the energy on the density  $E[\rho(r)]$  is not given by the Hohenberg-Kohn theorem, it is confirmed that such a functional exists [39].

Following the work of Kohn and Sham [41, 42], the approximate functional employed by current DFT method partition the electronic energy into several terms [4]:

$$E = E^T + E^V + E^J + E^{XC} \quad (2.70)$$

Where  $E^T$  is the kinetic energy term arising from the motion of the electrons,  $E^V$  includes terms describing the potential energy of the nuclear-electron attraction and of the repulsion between pairs of the nuclei,  $E^J$  is the electron-electron repulsion term, also described as the coulomb self-interaction of the electron density,  $E^{XC}$  is the exchange correlation term and includes the remaining part of the electron-electron interaction [31]. Note that all terms except the nuclear-nuclear repulsion are functional of the electron density  $\rho$  [4].  $E^{XC}$  is divided into exchange and correlation functionals, corresponding to the same spin and mixed-spin interactions, respectively:

$$E^{XC}(\rho) = E^x(\rho) + E^c(\rho) \quad (2.71)$$

The components on the right hand side of the equation above can be of different types: local functional density (local density approximation LDA) when the electron system has constant density ("homogenous electron gas"). In other words, local functional density depends only on the electron density, while a gradient-corrected functional (non-local) depends upon the gradient (or higher derivatives of  $\rho(r)$ ) for systems with varying density [20].

The local exchange functional (e.g. LDA) were developed to deduce the exchange energy of a uniform electron gas and thus has its shortcoming in describing molecular system [20]. In 1988, Becke formulated the gradient-corrected exchange functional based on the LDA exchange functional. It succeeded in remedying many of the LDA functional's deficiencies. Similarly, local (e.g. Vosko, Wilk, and Nusair) and gradient-corrected (Perdew) correlation functionals exist and are widely used. Pure DFT methods are defined by pairing an exchange functional with a correlation functional. For example, BP86, BLYP [32].

In practice, self-consistent Kohn-Sham DFT calculations are performed in an iterative manner analogous to the SCF procedure described for HF [32]. The density may be approximately written in terms of a set of auxiliary one-electron functions, so-called Kohn-Sham orbital, as

$$\rho(r) = \sum_i^N |\psi_i|^2 \quad (2.72)$$

The Kohn-Sham equations have the form [31]

$$\hat{h}_{ks} \psi_i = \varepsilon_i \psi_i \quad (2.73)$$

Where the operator

$$\hat{h}_{ks} = -\frac{1}{2} \nabla_1^2 - \sum_A \frac{Z_A}{r_{1A}} + \int \frac{\rho(2)}{r_{12}} dr_2 + V_{xc}(1) \quad (2.74)$$

Is similar to the Fock operator in the HF-approach. The corresponding potential  $V_{xc}(1)$  is given by a derivative of the energy  $E_{xc}$  with respect to the density  $\rho$  [43]

$$V_{xc}(1) = \frac{\partial E_{xc}[\rho]}{\partial \rho(r)} \quad (2.75)$$

According to the Gaussian user's reference, a Becke-style three-parameter functional (B3LYP: Becke 3 term, Lee Yang, Parr) may be defined via the following expression [1,4]:

$$E_{xc}^{B3LYP} = E_X^{LDA} + C_0(E_X^{HF} - E_X^{LDA}) + C_X E_X^{B88} + E_C^{VWN3} + Cc(E_C^{LYP} - E_C^{VWN3}) \quad (2.76)$$

Here the parameter  $C_0$  allows any mixture of HF and LDA local exchange. In addition, Beck's gradient correction to the LDA exchange is also included, scaled by the parameter  $C_X$ . Similarly, the VWN3 local correction function is used, and it may be optionally corrected by the LYP correlation correction via the parameter  $C_C$ . In the formulation of the B3LYP functional, the parameters were determined by fitting them to the atomization energies in the G1 molecule set, the values are:  $C_0 = 0.2$ ,  $C_X = 0.72$  and  $C_C = 0.81$ .  $E_{xc}$  cannot be evaluated analytically for DFT methods. Thus, in order to perform the numerical integration a grid of points in space must be employed. A crucial point in comparing different DFT-results based on the same functional is the quality of the chosen integration grid [4]. Density functional theory with gradient-corrected

exchange-correlation functional has proved to be a reliable tool to perform electronic structure calculations on transition metal complexes at a moderate cost [44, 45].

# Chapter 3

## Software Packages and Computational Methodology

### 3.1 Gaussian 98 Software

Computer programs which perform SCF (self-consistent field) calculations are widely available. The most common being those developed by J.A Pople and co-workers under the GAUSSIAN label [5]. Gaussian 98 [46] is a connected system of programs for performing a variety of semi-empirical and ab-initio molecular orbital (MO) calculations. The essential input data for such programs are the molecular geometry (including the specification of the constituent atoms), the basis set, the net charge of the system and the spin multiplicity. The output from such programs will consist of the total energy, the orbital energy and wave functions, and a population analysis [5].

Gaussian 98 is capable of predicting many properties of molecules and reactions, including [4]:

- Molecular energies and structures
- IR and Raman spectra
- Bond and reaction energies
- Energies and structures of transition states

- ☐ Vibration frequencies
- ☐ Thermo chemical properties
- ☐ Reaction pathways
- ☐ Molecular orbitals
- ☐ Atomic charges
- ☐ Multipole moments
- ☐ NMR shielding and magnetic susceptibilities
- ☐ Vibration circular dichroism intensities
- ☐ Electron affinities and ionization potentials
- ☐ Polarizabilities and hyperpolarizabilities
- ☐ Electrostatic potentials and electron densities

Computations can be carried out on systems in the gas phase or in solution, and in their ground state or in an excited state. Thus, Gaussian 98 can serve as a powerful tool for exploring areas of chemistry such as constituent effects, reaction mechanisms, potential energy surfaces, and excitation energies [4].

### **3.1.1 Running Gaussian 98**

The following steps are necessary to run Gaussian 98 in windows. (Gaussian also can be run in all the workstations and supercomputer versions):

- ☐ Start the program

- Load or enter Gaussian Input.
- Start execution of the job.
- Examine and interpret the output.

Start the program by double clicking on the Gaussian 98W icon. The main window is now open (Figure 3.1).

Provide the program with the inputs it need. The menu is used to create a new input file or to modify existing ones.

The route section specifies the procedure and basis set we want to use for the calculation ((Figure 3.2).

The title section of a Gaussian input file contains a description of the job.

The charge and multiplicity section of the input file specify the charge on the molecule and its spin multiplicity. Each one of them is entered as an integer with one space separating them. Spin multiplicity refers to the arrangement of electrons within the molecules. This is given by the equation  $2S+1$ , where S is the total spin of the molecule.

Molecular Specification section specifies the type and the position of each of the atom in the molecule: Gaussian accepts molecular specifications in several different formats:

**Cartesian coordinates:** Cartesian coordinate input consists of a series of lines of the form:

Atomic-symbol	X-coordinate	y-coordinate	z-coordinate
---------------	--------------	--------------	--------------

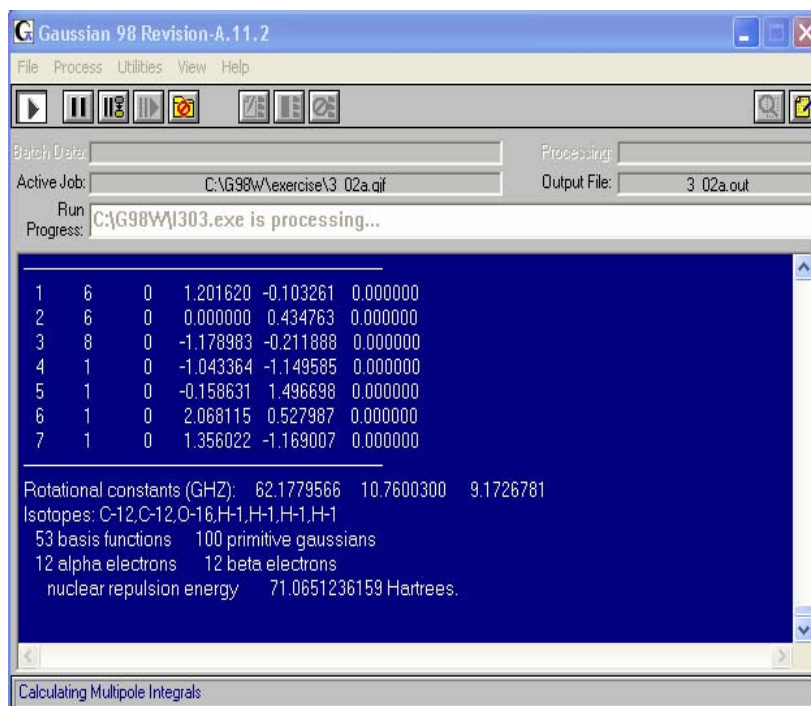


**Figure 3.1** Main program windows

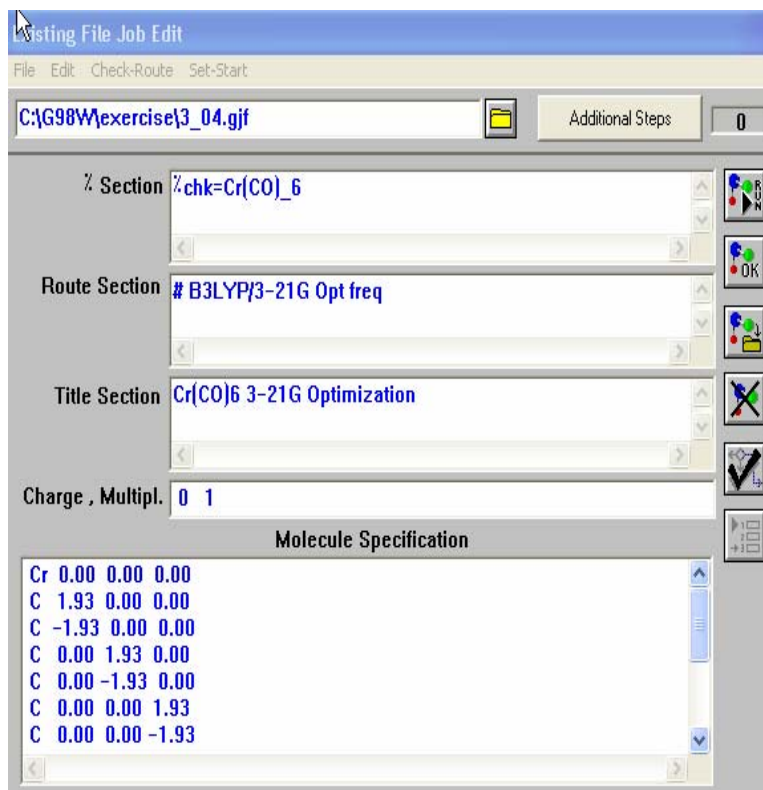


**Figure 3.2** Job entry windows

The molecular structure for  $\text{Cr}(\text{CO})_6$ , expressed in Cartesian coordinate is shown in Figure 3.3

```
0 1
Cr 0.00 0.00 0.00
C 1.93 0.00 0.00
C -1.93 0.00 0.00
C 0.00 1.93 0.00
C 0.00 -1.093 0.00
C 0.00 0.00 1.93
C 0.00 0.00 -1.93
C 3.07 0.00 0.00
C -3.07 0.00 0.00
C 0.00 0.00 3.07
C 0.00 0.00 -3.07
```

**Figure 3.3** Cartesian coordinates of  $\text{Cr}(\text{CO})_6$

**Z-matrix format ( internal coordinates):**

A Z-matrix specifies the locations of, and bonds between atoms using bond lengths, bond angles, and dihedral angles. Each atom in the molecule is described on a separate input line within the Z-matrix.

After the data entry, select run, and save the results from the file menu. When the program terminates the calculation, it will display "**normal termination of Gaussian 98W**". The output of the calculation is saved in the text file with the same name as you typed.

### 3.1.2 Using Gaussian Checkpoint

The Gaussian computational chemistry program allows the results of a calculation to be saved in a machine readable file, called a checkpoint file. This saved checkpoint file can be used for later use in another Gaussian 98 job for use by a visualization program to restart a failed job.

It is a good idea to make a backup copy of the check point files, because sometimes the checkpoint file will be corrupted while the program writes to it. Unless you specify a name for the checkpoint files, the program will delete this file at the end of successful run.

Gaussian will use a checkpoint file if the command

**Chk** = file-name

appears before the route section in the input file. If the specified file does not exist, the program will create it. In such case, the file will be saved in the current directory. But if one wants to save the file in alternative location,

the path of the directory where the checkpoints file to be saved must be specified.

### 3.1.3 Checkpoint File Utilities

**c8694** can be used to convert a checkpoint file from an old format to the Gaussian 98 format. It is given a single argument, which is the name of the checkpoint file. The file is overwritten by a new file with the same name.

**chkchk** is a utility provided with the Gaussian distribution. It extracts the title and route sections from a checkpoint file. The command usage is

**chkchk** file-name

where file-name.chk is the name of a checkpoint file in the current directory.

**chkmove** It is used to move checkpoint files between machines of different architecture.

## 3.2 Chem3D

Chem3D is an application designed to enable scientists to model chemicals. It combines powerful building, analysis, and computational tools with an easy-to-use graphical user interface, and a powerful scripting interface. Chem3D provides computational tools based on molecular mechanics for optimizing models, conformational searching, molecular dynamics, and calculating single point energies for molecules [47]

Chem3D can read a wide variety of popular chemical structure files, including Gaussian, Macro Model, MDL, MOPAC, PDB, and SYBYL. Two-dimensional structures imported from ChemDraw or ISIS/Draw is automatically converted to three-dimensional structures. The Chem3D native file format contains both the molecular structure and results of computations. Data can be exported in a variety of chemical-structure formats and graphics files.

Chem3D has both graphic and text-based structure-building modes. Structures can be generated graphically by sketching out the molecule. The builder creates carbon atoms, which can be edited by typing text to substitute other elements or functional groups. As the structure is built, the valence is filled with hydrogen atoms and typical bond lengths and angles are set. Several hundred predefined functional groups are available and users can define additional ones. The text-based mode allows the user to input a simple text string (similar to SMILES, but not identical). This text mode can be used to build structures entirely or to add functional groups [5].

### **3.2.1 Viewing Gaussian Structures with Chem3D**

With Chem3D, we can View the structures after a Gaussian calculation is terminated. In this procedure, use the Gaussian utility formchk to create a formatted checkpoint file. In the Chem3D file top menu select open. In the dialog box that appears select Gaussian Checkpoint. Then browse for the formatted checkpoint file created earlier and open.

### 3.3 Computational Details

The ab-initio and DFT calculations were performed using Gaussian 98 program. The model of the molecules is drawn by ChemDraw and Chem3D packages. Each figure is saved as PDB (protein data bank) file format, which can be opened by Gaussian Program to carry out the needed computation. The first stage of the Gaussian calculations was done using HF procedures. It involved geometry optimizations at HF/6-311G (D) and calculation of vibration frequencies. The geometry is reoptimized at DFT/6-311G(D), The Vibration frequencies of the carbonyls in molecules under study have been also calculated using the DFT/6-311G (D) to compare the results. All computations were run on Gaussian 98 as follows:

- Using the formchk Utility provided by Gaussian 98 to generate a formatted version of the checkpoint file which can be accepted by Chem3D.
- The optimized geometry of the complex is drawn by Chem3D, using the built in Gaussian job to create input file.
- This input file then entered to Gaussian to perform frequency calculations.
- Results of the calculations were interpreted using molcal package molecules. Harmonic vibration frequencies were calculated using the Hartree-Fock and density functional B3LYP (Becke's three

parameter exchange functional methods) [5], in combination with either the triple-split-valence polarized 6-311G\* or the LANL2DZ basis set. The 6-311G\* basis set was chosen since it has recently been extended to include the first row transition elements [5]. While the LANL2DZ basis set is available for many of the heavier elements. Thus, both the 6-311G\* and LANL2DZ basis sets can be used in calculations involving transition metal elements.

The issue which affects the calculations time is how the integrals are evaluated. There are several common methods:

- **Conventional Calculations** all the integrals are evaluated at the beginning of the calculations and stored in a file on a computer hard drive. This file is then accessed as the integrals are needed for each iteration of the self-consistent field calculation.
- **Direct Calculations** all the integrals are evaluated as they are needed and not stored at all.
- **In Core Calculation** an algorithm which computes all the needed integrals and then keeps them in ram memory rather than on a disk file.

In core calculations are always the fastest calculations because ram memory can be accessed much faster than the disk files.

### 3.4 Procedure

There are several procedures that can be carried out with any ab-initio program. We will restrict ourselves here to three:

⇒ Single point calculations

⇒ Geometry optimization

⇒ Frequency calculations

#### 3.4.1 Single Point Calculations

In this procedure, energy, wave function, and other requested properties at a single fixed geometry can be calculated. This procedure is normally done for new molecules to check the nature of the wave function, and hence to start the geometry optimization from this point. Single point calculations also can be used to compute very accurate values of the energy and other properties of the molecule which has been optimized at a lower level of theory. Single point calculations can be performed at any level of theory with small or large basis sets [4].

#### 3.4.2 Geometry Optimization

Geometry Optimization is a technique used by computational chemists to minimize the molecule energy iteratively using geometric approximations. A small change in the structure of the molecule will produce a difference in its energy and other properties [4]. Geometrical optimization seeks to minimize the potential energy surface. "A potential energy surface is a mathematical relationship linking molecular structure

and the resulting energy". The way the energy of a molecule system varies with small changes in its structure is specified by its potential energy surfaces. For a diatomic molecule, the potential energy surface is a two dimensional plot with the internuclear separation on the x axis". (See Figure 3.4) [4].

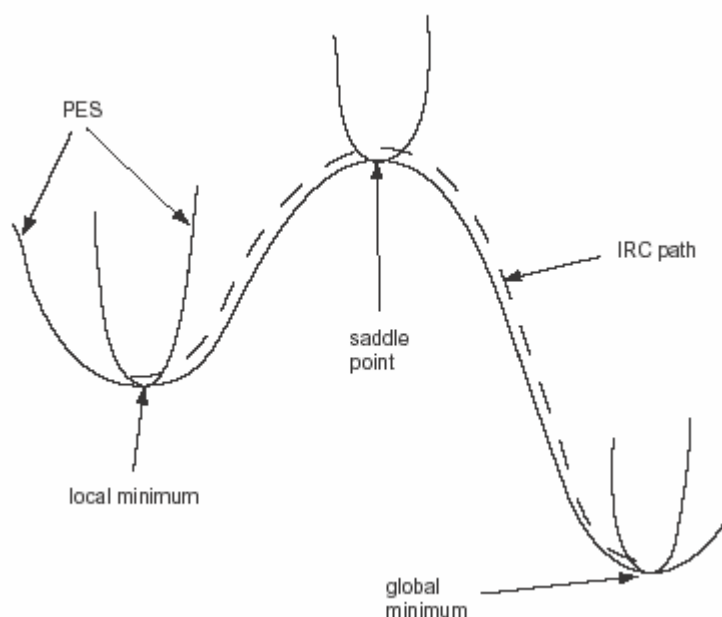


**Figure 3.4** Potential energy surfaces

This sort of drawing considers only one degree of freedom within the molecule. There are two minima on this potential surface. A minimum is the bottom of a valley on the potential surface. A minimum can be a local minimum or a global minimum.

A geometry optimization begins at the molecular structure specified as the input. The energy and the gradient are computed at that point. The step size directions along the potential energy surface are determined for the next step [4].

### **Preparing Input for Geometry Optimizations**

The **Opt** keyword in the route section requests a geometry optimization. This is done using the basis set and a level of theory specified by other key words.

#### **3.4.3 Optimization Algorithm**

There are many different algorithms for finding the set of coordinates corresponding to the minimum energy. These are called optimization algorithms because they can be used equally well for finding the minimum or maximum of a function. If only the energy is known, then the simplest algorithm is one called the simplex algorithm. This is just a systematic way of trying larger and smaller variables for the coordinates and keeping the changes that result in a lower energy. Simplex optimizations are used very rarely because they require the most CPU time of any of the algorithms discussed here. A much better algorithm to be used when only energy is known is the Fletcher-Powell (FP) algorithm. This algorithm builds up an internal list of gradients by keeping track of the energy changes from one step to the next. The Fletcher-Powell algorithm is usually the method of choice when energy gradients cannot be computed. If the energy and the gradients of energy can be computed, there are a number of different algorithms available. Some of the most efficient algorithms are the quasi-Newton algorithms, which assume a quadratic potential surface. One of the most efficient quasi-Newton algorithms is the Broyden algorithm, which internally builds up a second derivative Hessian

matrix. Steepest descent and scaled steepest descent algorithms can be used if there is not a reasonable assumption [48]. Another good algorithm is the geometric direct inversion of the iterative subspace (GDIIS) algorithm. Molecular mechanics programs often use the conjugate gradient method, which finds the minimum by following each coordinate in turn, rather than taking small steps in each direction. The Polak-Ribiere algorithm is a specific adaptation of the conjugate gradient for molecular mechanics problems. Algorithms using both the gradients and second derivatives (Hessian matrix) often require fewer optimization steps but more CPU time due to the time necessary to compute the Hessian matrix. In some cases, the Hessian is computed numerically from differences of gradients.

These methods are sometimes used when the other algorithms fail to optimize the geometry. Some of the most often used are eigenvector following (EF), Davidson-Fletcher-Powell (DFP), and Newton-Raphson [5].

#### **3.4.4 Frequency Calculations**

The vibration states of the molecules can be observed by infrared and Raman spectroscopy, which can help in determining the molecular structure. But for large molecules, there is difficulty due to large number of closely spaced peaks. To overcome this problem, computer simulation is used to calculate the vibration frequencies of molecules. We carry out frequency calculations for different purposes [4]:

- ⇒ To predict IR and Raman spectra of molecules (frequency and intensities).
- ⇒ To compute force constants for a geometry optimization.
- ⇒ To identify the nature of stationary points on the potential energy surface.

When the calculation are performed to compute the Energy and to optimize the geometry, the quantum chemical programs ignore the vibrations in molecular systems [4]. In this approach, the computations consider an idealized view of nuclear position. In reality, the nuclei in the molecules are constantly in motion. In equilibrium states, these vibrations are regular and predictable since molecular frequencies depend on the second derivatives of the energy with respect to the nuclear position. The molecules can be identified by their characteristic spectra.

Frequency calculations are valid only at stationary points on the potential energy surface. Thus, frequency calculations should only be carried out at the geometry obtained from an optimization run and with the same basis set and method. Any other calculation will give meaningless results [4].

### **Input for Frequency Jobs**

In order to carry out frequency calculations, you have to include the **Freq** keyword in the route section. The other sections of the input files are the same as those considered for geometry optimization.

## Chapter 4

### Reactivity and Bonding of Metal Carbonyl Complexes

#### 4.1 Introduction

The discovery of  $\text{Ni}(\text{CO})_4$  in 1890 by Mond, Carl Langer and Quinke by accident [49], started chemical research which led to the preparation of a large number of metal carbonyls, such as  $\text{Fe}(\text{CO})_4$ ,  $\text{Fe}(\text{CO})_9$ ,  $\text{Mo}(\text{CO})_6$ ,  $\text{W}(\text{CO})_6$  and  $\text{Cr}(\text{CO})_6$  in recent years [10]. Metal carbonyls are compounds in which a bond exists between a carbon atom of the carbonyl group and a transition metal. They play a very important role in chemistry and chemical industry. This field which combines aspects of organic and inorganic chemistry has many important applications [8]. For example,  $\text{Fe}(\text{CO})_5$  was used as an anti-knock agent in motor fuels. Even though lead tetraethyl is a better anti-knock agent, iron carbonyl is less poisonous [10]. The transition metals have partially filled d or f orbitals. They react with a variety of molecules or groups, called ligands, to form transition metal complexes. In forming a complex, the ligands donate electrons to vacant orbital of the metal. The bond strengths between the metal and the ligand range from very weak to very strong [8]. Studying the effect of the ligands on the reactivity of the metal complex plays a central role in inorganic chemistry, since changing the ligand bonded to the metal

will change the complex reactivity [10]. A well-known feature of metal carbonyls is that they are more stable when they have the electronic configuration of a noble gas, i.e., the total number of electrons around the metal is 36, 54, or 86 corresponding to the atomic numbers of the noble gases Kr, Xe, and Rn. In this case the metals are said to have the effective atomic number of the noble gases or to obey the 18-electron rule [10].

## 4.2 Carbonyl Complexes

Organometallic chemistry plays an important role in industry and medicinal fields [49]. Carbonyl complexes are compounds that contain carbon monoxide as a coordinated ligand. Carbon monoxide is a ligand that forms complexes with most transition metals [50]. Carbon monoxide does form strong bonds to transition metals; this is due in part to the synergistic nature of its bonding to transition metals [18]. To consider why carbon monoxide forms such a strong bond, let us look at its structure and the bonding orbital: The nature of the carbonyl bonding to the metal and related complexes can be described as consisting of two components:

- The carbonyl group possesses a  $sp$ -hybrid lone pair of electrons which will form  $\sigma$ -bond by the overlap with the transition metal  $d$  orbital as shown in Figure 4.1 [10].
- The excess electron density around the metal center is donated back to the empty orbital of the CO which is called  $\pi$  Back-bonding as shown in Figure 4.2.  $\sigma$  and  $\pi$  bonding reinforces each other.

Back-bonding is important when the metal has many electrons to dissipate, which make the low oxidation state of the metals stabilized by back-donation to the ligand [50].



**Figure 4.1**  $\sigma$ -bonding, orbitals overlap in M-CO bonding. Arrow shows direction of electron flow, ligand to metal  $\sigma$  bonding

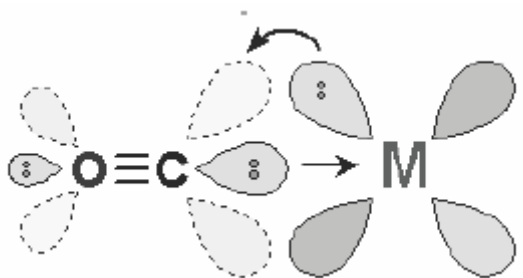


**Figure 4.2**  $\pi$  back-bonding. Metal-to-ligand  $\pi$  back-bonding.

The two components of this bonding are synergistic. The more sigma donation by the carbonyl or other sigma-donors on the metal center, the stronger the  $\pi$  back-bonding interaction. Notice that although this involves the occupation of an  $\pi^*$  orbital on the CO, it is still a bonding interaction as far as the metal center is concerned. It is generally understood that the decrease in vibration frequency of CO on metal carbonyl is due to  $\pi$  back-donation from d-block metals, leading to a weak C-O bond [49]. In other words, the IR absorbances of metal carbonyl are strongly affected by changes in electronic structure at the

transition metal center. This hypothesis was based on CO stretching frequency, where there is a decrease in the vibration frequency of CO on metal carbonyl. This decrease is due to  $\pi$  back-donation from d-block metal which causes a reduction in the bond order of C-O [49, 50].

### 4.3 Phosphine Ligands

Phosphine ligands have the general formula  $\text{PR}_3$ , where R = alkyl, aryl, H, halide etc. Phosphine ligands are neutral two electron donors that bind to transition metals through their lone pairs. In addition, phosphine forms  $\pi$  back-bonding to the metal. For example, the  $\text{PCl}_3$  group is an electron attracting

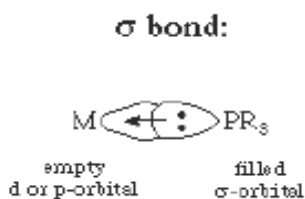


**Figure 4.3**  $\sigma$  donating of the phosphine lone pair to an empty metal orbital

group because it is a good  $\pi$  acceptor [50]. The bonding between the phosphine ligands and metals is like the bonding between carbonyl ligands and metal. This bond has two components:

- The primary component is sigma donation of the phosphine lone pair to an empty orbital on the metal as shown in Figure 4.3.

- The second component is back donation from a filled metal orbital to an empty orbital on the phosphine ligand as shown in Figure 4.4 [50].

In general, the electronic properties of the ligands depend on their molecular parts. Changing the molecular parts of a ligand change its electronic properties. Strohmeier showed that phosphorus ligands can be arranged in a series based on the CO stretching frequencies [10]. His

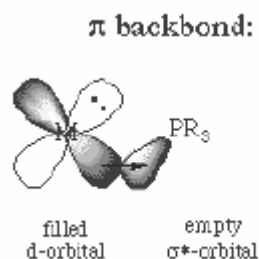
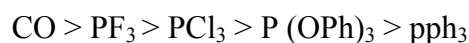
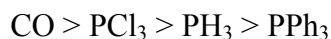


**Figure 4.4** Back donations from a filled metal orbital to an empty d orbital on the phosphine ligand

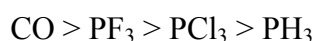
arrangement was based on the hypothesis that the CO stretching frequency depends upon the CO bond order which depends upon the nature of other ligands bonded to the metal center. As the ligand donates electrons to the metal center, the metal donates electrons to the CO  $\pi^*$  orbital causing a reduction in the CO bond order and hence a reduction in the IR stretching frequency [49, 50]. For example, Horrocks and Taylor described a series of ligands according to their ability of  $\pi$  acceptor. Some of these ligands are listed below [10]



According to the X-ray crystallographic and infrared data, the order of decreasing  $\pi$ -acceptor ability is [51]:



From the above discussion, we can conclude that the trend of the order of  $\pi$  back bonding ability is



Some ligands have no  $\pi$  acceptor properties. They do have  $\sigma$  donating properties. For example, nitrogen in amine and oxygen in ether [10]. Clearly, different ligands have different electronic properties. This causes them to bond differently to the metal center. As shown earlier the carbonyl bond by both  $\sigma$  bonding and  $\pi$  back-bonding. However, there is a great deal about the nature of back bonding of phosphines with transition metals. The empty phosphorous orbital which accept the electrons from the metal filled d orbital which known as  $\pi$  back-bonding has been described as being either a d-orbital or an anti-bonding  $\sigma$  orbital. In the  $\text{PX}_3$  systems with  $\text{X} = \text{H}, \text{CH}_3,$  or  $\text{F}$ , Marynick's [52] molecular orbital calculations indicated that  $\pi$ -acceptor orbital on phosphorus mostly consists of phosphorus 3p character, i.e. the back bonding takes place through the  $\sigma^*$  orbital of the sigma\* of P-X bond for ligands such as  $\text{PF}_3$  and  $\text{PH}_3$ . By studying a series of complexes of the type  $\text{RCr}(\text{CO})_5$ , with  $\text{R} = \text{H}, \text{CH}_3,$   $\text{PH}_2,$   $\text{OH}$ , using ab-initio calculation and density functional calculations, Creve, Pierloot, Nguyen and Vanquicken borne showed that one p orbital, perpendicular to the P-R bond and doubly occupied, is used to form a  $\sigma$

bond with the empty d orbital of the  $\text{Cr}(\text{CO})_5$  fragment. The remaining p orbital of PR is suitable to  $\pi$  back-bonding with the occupied d(Cr) orbital [53]. The donor and acceptor of these ligands are influenced by the identity of R [50]. When the R group in the phosphine ligands is an electron-withdrawing (electronegative) groups, the  $\sigma$ -donating capacity of the phosphine ligand to the metal tends to decrease, and the  $\pi$ -back bonding ability is promoted by electron withdrawing groups such as F and Cl [50]

#### **4.4 Trans-Effect (TE)**

##### **4.4.1 Introduction**

The idea of Trans-influence and the related Trans-effect are crucial in modern inorganic chemistry. A coordinate ligand can exert a profound influence upon the metal-to-ligand bonding and stability of other ligands within a complex, particularly those in a trans position to this ligand [54]. The majority of work on TE was concentrated on square planar complex. The Trans-effect in octahedral complexes is not as well explained as in the square planar complexes and will be discussed right now.

##### **4.4.2 Background**

One of the first theoretical descriptions of TE was the polarization theory suggested by Grinberg in 1932 [54]. This theory state that a build up of negative charge on the metal induced by the polarizable donor group repels the negative charge in the trans ligand, and weakens the trans bond.

In 1948, Syrki explain the TE differently. He included hybridization at the metal, in which he suggested that opposing metal-ligand bonds will compete for the available s and d orbitals. The early theoretical treatments of TE considered only  $\sigma$ -bond. Later, Orgel took into account metal-ligand  $\pi$ -bonding [54]. But when  $\pi$  back-bonding was taken into account, it must be noted that not all metals will be able to make  $\pi$ -back bonding such as Nd. Orgel explained this by invoking transition state stabilization by such  $\pi$ -acceptor ligands. In 1969, Bright Ibers invoked steric effects where the structure of the complex is strongly affected by the steric repulsion of the cis ligand. Tolman has shown that the steric and electronic properties ligands influence reactivity of transition metal complexes [54]. The effect of the steric properties on the reactivity of metal carbonyl result from non-bonding forces between parts of the molecule. Changing the ligands will change the molecule electronic properties which affects the electronic properties [10]. It's now clear that a complete understanding of TE must account for both electronic effects an also, steric factors. The former require consideration of both  $\sigma$  and  $\pi$  back-bonding properties of both the metal center and ligands, while the later are usual most important for ligands which are cis to each other. The presence of certain ligands trans to a leaving ligand in a substitution reaction lowers the activation energy relative to that when other ligand is in the trans position. The lowering can be accomplished in either of two ways:

- By raising the energy of the reactant's ground state
- Or by lowering the energy of the transition state

Good Trans-directing ligands must act in on both of these ways [50].

#### **4.4.3 Structural Trans-effect (STE) In Octahedral Metal Complexes**

The Trans-influence also termed Structural Trans-effect, describes the ability of a ligand to weaken (and lengthen) the bond trans to it in preference to those in cis position [54]. It is known that the Trans-influence is a ground state effect [50]. In other words, STE depends on the electronic properties of the ligand bonded to the metal. The better donor ligand will stabilize the transition state and therefore increase the rate of dissociation of the trans ligand [10]. Better  $\pi$ -acceptor ligands reduces the bonding between the ligand trans to it and the metal center. So there is reversibly relation between the bonding of the ligand and the metal, and the trans ligand and the metal. As the  $\pi$ -acceptor of the ligand increases, the electron density between the trans ligand and the metal center decreases. This weakens the bond between the trans ligand and the metal, resulting in an increase in the rate of trans ligand dissociation [10].

#### **4.5 Kinetic Trans-effect (KTE) in Octahedral Metal Complexes**

Although a STE destabilizes a complex in the ground state, this will enhance reactivity towards ligand substitutions only if there is no effect on the energy of the transition state. This is sometimes the case for dissociative activated substitutions. The STE and KTE ligand series of a

particular complex will then be similar. However, if the transition state energy is affected by the ligand in question, then there may be no correlation between STE and KTE. In other words, when the ligand has a donating ability, the transition state will be stabilized, and the activation energy will be decreased, only then will the KTE be dominated [54].

## Chapter 5

### Results and Discussion

#### 5.1 Structure and Energy of Cr (CO)<sub>6</sub>

In this section, a detailed analysis of the energetics and electronic structure of Cr(CO)<sub>6</sub> were carried out using HF and DFT methods with various basis sets. The results of these calculations are compared with the reported experimental values [55]. Table 5.1 shows the predicted Cr-CO and C-O bond lengths of the ground state geometries of Cr(CO)<sub>6</sub> obtained by HF calculations using different basis sets, together with the experimental values. The optimized structure is shown in Figure 5.1

**Table 5.1** Theoretical predictions of total energies, and bond length of Cr(CO)<sub>6</sub> at HF level of theory with various basis sets

Model	r(Cr-CO) Å	r(CO) Å	Energy (Hartree)
HF/STO-3G	1.79	1.17	-743.40
HF/3-316G	1.93	1.13	-1710.78
HF/6-311G	2.078	1.145	-743.40
HF/6-311G(D)	2.002	1.112	-1719.77(-1719.852) <sup>c</sup>
HF/LANL2DZ	2.078	1.145	-743.40
Exp	1.92 <sup>a</sup>	1.141 <sup>b</sup>	

<sup>a</sup>[55], <sup>b</sup>[55], <sup>c</sup>[7]

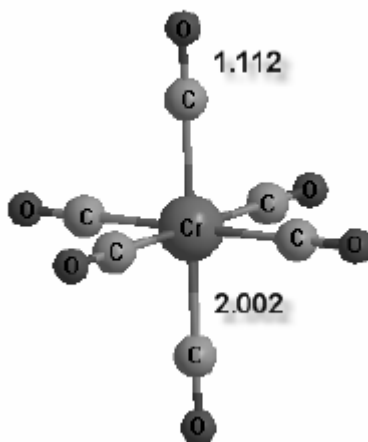


**Figure 5.1** Optimized Structure of  $\text{Cr}(\text{CO})_6$  at HF/6-311G(D), bond length is in Å.

The results in Table 5.1 show HF is not adequate. This is due to lack of electron correlation. Table 5.2 shows the Cr-CO and C-O bond lengths obtained by DFT calculations using different basis sets, together with the experimental values. The optimized structure is shown in Figure 5.2.

**Table 5.2** Theoretical predictions of total energies, and bond length of  $\text{Cr}(\text{CO})_6$  at DFT with various basis sets

Model	$r(\text{Cr-CO})$ Å	$r(\text{CO})$ Å	Energy (Hartree)
B3LYP/3-21G	1.881	1.165	-1715.80
B3LYP/6-31G	2.078	1.145	-743.40
B3LYP/6-311G(D)	1.922	1.141	-1724.74 (-1722.649) <sup>b</sup>
EXP	1.92 <sup>a</sup>	1.141 <sup>a</sup>	

<sup>a</sup>[55], <sup>b</sup>[7]

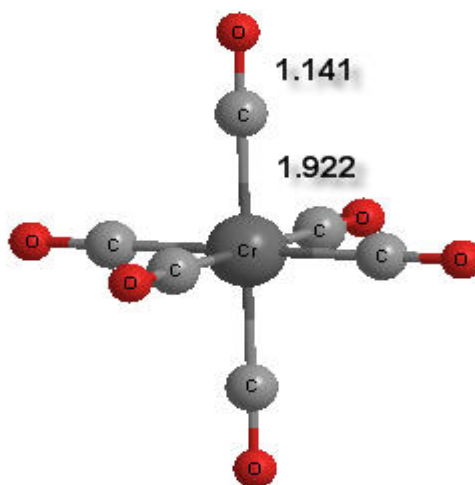


**Figure 5.2** Optimized Structure of  $\text{Cr}(\text{CO})_6$  at DFT/6-311G(D), bond length is in Å

The calculated  $r(\text{CO})$  bond length values in Table 5.2 indicate that the maximum deviation of the calculated values from the experimental data is 0.004 Å when the 6-31G basis set is used. The observable effect occurred in the right direction when 6-311G(D) basis set is used, shortening the CO bond by 0.004 Å.

Clearly from Table 5.1 and Table 5.2, the geometry obtained with DFT method are in reasonable agreement with those reported experimentally. It is clear from Table 5.2 that DFT level of theory with triple-split-valence polarized 6-311G (D) basis set produces much better results than the other basis set. Accordingly, in the rest of this work, DFT level of theory, with 6-311G (D) basis set will be used.

## 5.2 Predicted Geometry of Cr(CO)<sub>5</sub>pip

The geometry of the Cr(CO)<sub>5</sub>pip and vibration frequencies were calculated using DFT combined with different basis sets. Table 5.3 shows the predicted geometry of the optimized structure, and Figure 5.3 shows the optimized structure.

**Table 5.3** Optimized structure of Cr(CO)<sub>5</sub>pip and the corresponding energy parameter using DFT with different basis sets

Model	r(Cr-N) Å	r(Cr-CO)(trans) Å	CO(trans)	CO(cis)
B3LYP/6-311G(D)	2.285	1.864	1.151	1.147
B3LYP/LANL2DZ	1.256	1.858	1.183	1.18
B3LYP/3-21G	2.214	1.822	1.174	1.172

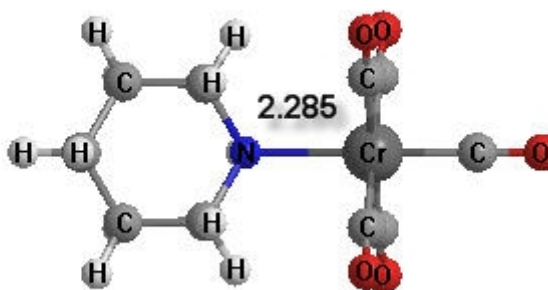


**Figure 5.3** Optimized structure of Cr(CO)<sub>5</sub>pip using DFT with 6-311G(D)

The trans CO bond length in the optimized structure of Cr(CO)<sub>5</sub>pip using DFT with 6-311G(D) equals 1.151 Å. This is greater than the

corresponding bond length in  $\text{Cr}(\text{CO})_6$  (1.141 Å) optimized structure at the same level of theory with the same basis set. Also the trans Cr-CO bond length in  $\text{Cr}(\text{CO})_5\text{pip}$  equals 1.864 Å. This is smaller than the corresponding bond length in  $\text{Cr}(\text{CO})_6$  (1.922 Å). This result can be explained as follows: Since pip is an electron donor to the metal, the metal center becomes electron-rich. The metal will then donate electrons to the trans CO as  $\pi$  back-bonding. This will strengthen the bond between the metal and CO, and decrease the bond between the C and O. This result can be seen from a different point of view, by comparing the vibration frequencies of CO in both compounds. The experimental  $\nu\{\text{CO}\}$ s for  $\text{Cr}(\text{CO})_6 = 2000 \text{ cm}^{-1}$ , and the calculated  $\nu\text{CO}$  for the trans CO in  $\text{Cr}(\text{CO})_5\text{pip} = 1941 \text{ cm}^{-1}$ , and  $1944 \text{ cm}^{-1}$ . This decrease in vibration frequencies for the trans CO in  $\text{Cr}(\text{CO})_5\text{pip}$  is due to the  $\pi$  back-donation from d-block metal.

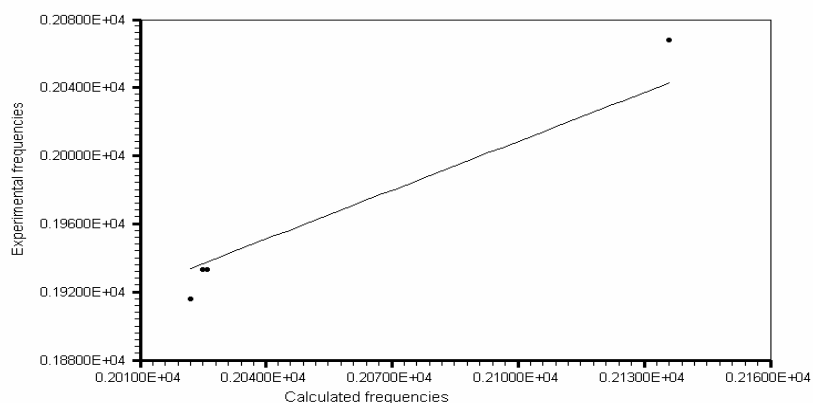
### 5.3 Vibration Frequencies for $\text{Cr}(\text{CO})_5\text{pip}$

Table 5.4 shows raw vibration frequencies, computed at the DFT level of theory with 6-311G (D) basis set with the corresponding intensity. Raw frequencies computed at the HF, DFT contain known systematic error due to the neglect of electron correlation. Therefore it is usual to scale frequencies predicted at HF, DFT by an empirical factor. A typical scale factor for DFT calculation is 0.96 [4].

**Table 5.4** Calculated frequencies of trans CO in Cr(CO)<sub>5</sub>pip at B3LYP with 6-311G(D)

Calculated IR	Intensity
2136 $A_1^{(1)}$	91
2025 E	1910
2026 E	1894
2022 $A_1^{(2)}$	950

The scale factor will vary from one basis set to another. In this study, a constant scale factor will be used with  $y = mx$  where  $m$  is the slope of the line,  $x$  take its value from the calculated frequencies and  $y$  is the scaling frequencies. This scale factor can be derived from running out a linear regression on all data points, while forcing the regression line through the origin (0,0). In other words, constant scale factor is the slope of the line which fit the experimental frequencies to the calculated frequencies at a given basis set, Figure 5.4. The data obtained using DFT with 6-311G (D) will be used in this process. There are many packages which can do this such as Excel, Lab Fit programs. Here, Lab fit program will be used. The computed scale factor is 0.960. As a result, the scaled frequencies vs the experimental frequencies are given in Table 5.5



**Figure 5.4** Experimental data vs. B3LYP data with applied scale factor

**Table 5.5** Unscaled frequencies, scaled frequencies, intensity, experimental frequencies of CO in Cr(CO)<sub>5</sub>pip

Unscaled frequencies	IR intensity	Scaled frequencies	Exp <sup>a</sup>
2136 $A_1^{(1)}$	91	2050 $A_1^{(1)}$	2068 $A_1^{(1)}$
2025 $E$	1910	1944 $E$	1933 $E$
2026 $E$	1894	1945 $E$	
2022 $A_1^{(2)}$	950	1941 $A_1^{(2)}$	1916 $A_1^{(2)}$

<sup>a</sup>[57]

It is clear that the density functional theory gives good correlation with experimental data.

#### 5.4 Structure and Properties of ( $\eta^1$ -chlorobenzene)Cr(CO)<sub>5</sub>

In this section, the ground-state geometry of ( $\eta^1$ -chlorobenzene)Cr(CO)<sub>5</sub> had been optimized using DFT level of theory, with the 6-311G(D) basis set. The optimized structure of this compound is shown in Figure 5.5. The selected optimized parameters are given in Table 5.6. From Table 5.2, the bond length between Cr and CO in the optimized structure of Cr(CO)<sub>6</sub> at DFT/6-311G(D) equals 1.922 Å, whereas the bond length between C and O equals 1.144 Å.

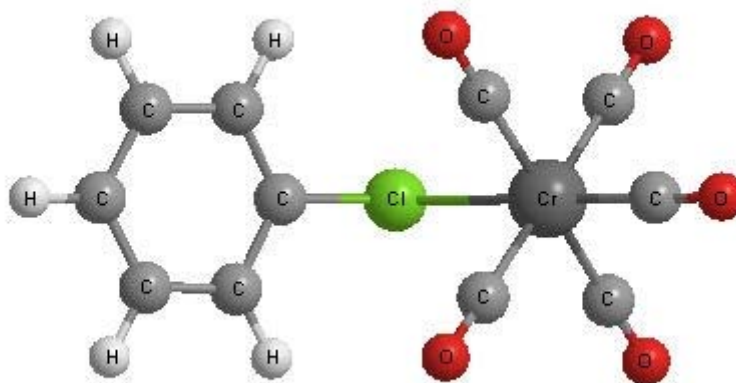


**Figure 5.5** The optimized structure of the ( $\eta^1$ -chlorobenzene)Cr(CO)<sub>5</sub> using DFT with 6-311G(D) basis set

**Table 5.6** Theoretical predictions of the bond length of ( $\eta^1$ -chlorobenzene)Cr(CO)<sub>5</sub> using DFT level of theory with 6-311G(D) basis set

	bond length Å
Cr-Cl	2.658
Cr-CO <sub>a</sub>	1.835
Cr-CO <sub>b</sub>	1.916
C-O <sub>c</sub>	1.15
C-O <sub>d</sub>	1.144

a; trans CO, b; average bond length of cis CO, c; trans CO, d; average bond length of cis CO

When one of the CO is replaced by CB, (Figure 5.6), the bond length between Cr and the trans CO equals 1.853 Å. The bond length between C and O in the trans carbonyl equals 1.15 Å. This decrease of the trans Cr-CO bond length and increase in the trans CO bond length in ( $\eta^1$ -chlorobenzene)Cr(CO)<sub>5</sub> is due to  $\pi$  back-donation to the trans CO. Since CB donates its electrons in the halogen to the metal, the metal center becomes electron-rich, and to compensate for this, it will donate electrons to the trans CO as  $\pi$  back-bonding. This will strengthen the bond between the metal and CO, and decrease the bond between the C and O in the trans CO. The CB ligand also enhances Cr-CO back-bonding to the equatorial CO ligands (Figure 5.6). This results in equatorial Cr-CO bond lengths that

are slightly shorter in ( $\eta^1$ -chlorobenzene)Cr(CO)<sub>5</sub> (1.916 Å) than in Cr(CO)<sub>6</sub> (1.922 Å).

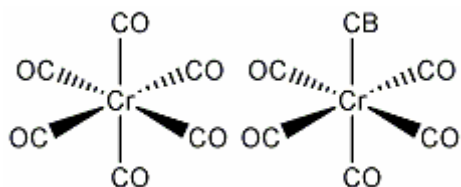


**Figure 5.6** Schematic representation of Cr(CO)<sub>6</sub> and Cr(CO)<sub>5</sub>CB

By comparing the vibration frequencies of CO in both compounds. The carbonyl stretching frequencies in ( $\eta^1$ -chlorobenzene)Cr(CO)<sub>5</sub> are 1939 cm<sup>-1</sup>, 1954 cm<sup>-1</sup>, 1955 cm<sup>-1</sup>, 1981 cm<sup>-1</sup>. These values are lower than the carbonyl stretching frequency in Cr(CO)<sub>6</sub> which is equal to 2000 cm<sup>-1</sup>, this indicates that the CO bond length in ( $\eta^1$ -chlorobenzene)Cr(CO)<sub>5</sub> is stronger and shorter than the corresponding one in Cr(CO)<sub>6</sub>.

#### 5.4.1 Carbonyl Frequencies of ( $\eta^1$ -chlorobenzene)Cr(CO)<sub>5</sub>

For the carbonyl frequencies of the Cr(CO)<sub>5</sub>CB, the program gives 4 values which are given in the Table 5.7 with the corresponding IR intensity, and the experimental values.

One of the calculated frequencies is doublet and the other two are singlet. These values are in agreement with the metal carbonyls IR active modes of the mono substituted. Figure 5.7 shows the possible stretching mode of vibrations for several metal complexes. For example, Table 5.7 shows that for monosubstituted metal carbonyl, there are four active modes, one is

doublet and the other two are singlet. We can see from Table 5.7 that the two frequency values  $2044\text{ cm}^{-1}$ , and  $2045\text{ cm}^{-1}$  have 1763, 1895 IR intensity values, respectively. These two values which have the highest IR intensity corresponding to the available doublet experimental value obtained by applying pulsed laser flash photolysis with visible and infrared detection ( $1958_{\text{vs}}\text{ cm}^{-1}$ ) [11]. The other calculated singlet value ( $2029\text{ cm}^{-1}$ ) with an IR intensity (984) corresponding to the experimental frequency ( $1934_{\text{m}}\text{ cm}^{-1}$ ). Dobson and co-workers were unable to see the IR stretching frequency ( $2070\text{ cm}^{-1}$  or scaled  $1979\text{ cm}^{-1}$  [11]. Our calculations indicate that this missing IR frequency has a very low IR intensity.

As presented in section 5.3, because of the error in the computation, the calculated frequencies given in Table 5.7 must be scaled with a scale factor. This scale factor was calculated using linear regression with Lab Fit program. The carbonyl frequencies of ( $\eta^1$ -chlorobenzene)  $\text{Cr}(\text{CO})_5$  will be used to calculate the scaling factor because only the experimental values of the frequency ( $\eta^1$ -chlorobenzene) $\text{Cr}(\text{CO})_5$  were available. After running linear regression with LAB FIT, the scale factor obtained was 0.956. Figure 5.8 shows the fitting between the experimental and the computed frequency from which the scale factor was calculated.

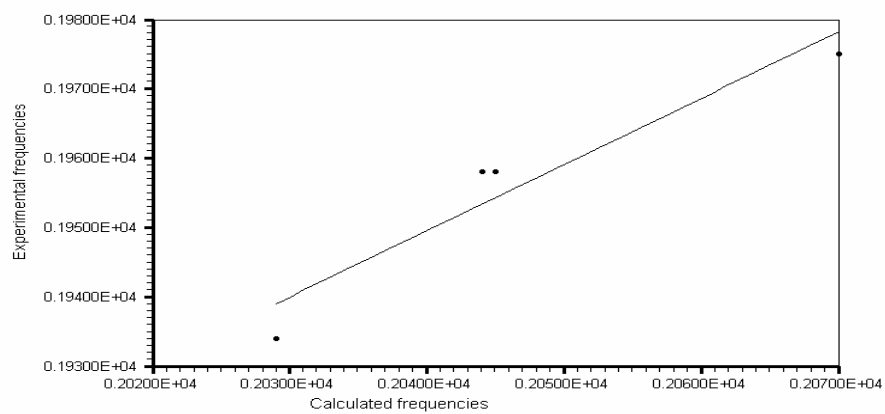


Figure 5.8 Experimental data vs. B3LYP data with applied constant scale factor

Complex		Point group	Symmetry of IR-active CO normal modes	Number $\nu_{CO}$ expected
1. $M(CO)_6$		$O_h$	$T_{1u}$	1
2. $M(CO)_5L$		$C_{4v}$	$A_1 + E (+A_1)$	2 or 3
3. $M(CO)_4L_2$	<i>trans:</i>	$D_{4h}$	$E_u$	1
	<i>cis:</i>	$C_{2v}$	$A_1 + B_1 + B_2 + (+A_1)$	3 or 4
4. $M(CO)_3L_3$	<i>mer:</i>	$C_{2v}$	$2A_1 + B_2$	3
	<i>fac:</i>	$C_{3v}$	$A_1 + E$	2
5. $M(CO)_5$		$D_{3h}$	$A_2'' + E'$	2
6. $M(CO)_4L$	<i>ax:</i>	$C_{3v}$	$2A_1 + E$	3
	<i>eq:</i>	$C_{2v}$	$2A_1 + B_1 + B_2$	4

Figure 5.7 Infrared active modes of metal carbonyls, Ref [50]

The scaled frequency vs. the experimental frequency is given in the Table 5.7.

**Table 5.7** Calculated unscaled frequencies, scaled frequencies, IR intensity and experimental frequencies in  $\text{cm}^{-1}$  of ( $\eta^1$ -chlorobenzene) $\text{Cr}(\text{CO})_5$  using DFT level of theory with 6-311G (D) basis set.

Unscaled Fre	IR intensity	Scaled Freq	Exp <sup>a</sup>
2029 $A_1^{(1)}$	984	1939 $A_1^{(1)}$	1934 $A_1^{(1)}$
2044 $\epsilon$	1763	1954 $E$	1958 <sub>vs</sub>
2045 $E$	1895	1955 $E$	1958 <sub>vs</sub>
2070 $A_1^{(2)}$	69	1981 $A_1^{(2)}$	.... $A_1^{(2)}$

<sup>a</sup>[11]

It's clear from Table 5.7 that there is a good agreement between the experimental data, and the calculated data, which again prove that DFT method is a good method for such compounds.

### 5.5 Structure and Properties of $\text{trans}-(\text{CB})(\text{L})\text{Cr}(\text{CO})_4$ Complexes, where L = CO, $\text{PH}_3$ , $\text{PCl}_3$ and $\text{PF}_3$

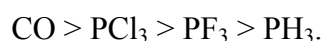
In this section we will study, by theoretical means, the electronic properties of  $\text{trans}-(\text{CB})(\text{L})\text{Cr}(\text{CO})_4$ , where L = CO,  $\text{PH}_3$ ,  $\text{PCl}_3$  and  $\text{PF}_3$  to study the nature of bonding of CB with the metal center in this case chromium which was shown to take place between the chlorine and chromium [11,12], and the effect of these ligands on the bond between

(CB) and Chromium. The data in Table 5.8 show the effect of the ligands  $L = \text{CO}, \text{PH}_3, \text{PCl}_3$  and  $\text{PF}_3$ , on the Cr-CB bond in the series of the compounds  $\text{trans}-(\text{CB})(\text{L})\text{Cr}(\text{CO})_4$ .

**Table 5.8** Optimized parameters (bond length Å) of  $\text{trans}-(\text{CB})(\text{L})\text{Cr}(\text{CO})_4$  where  $L = \text{CO}, \text{PH}_3, \text{PCl}_3$  and  $\text{PF}_3$  using DFT with 6-311G(D) basis set

L trans to CB	Cr-CB	Cr-P	Cr-COcis	Cr-COtrans	COcis	COtrans
CO	2.658		1.916	1.853	1.144	1.15
$\text{PCl}_3$	2.642	2.189	1.910		1.143	
$\text{PF}_3$	2.633	2.156	1.910		1.144	
$\text{PH}_3$	2.619	2.305	1.900		1.150	

The affect of these ligands on Cr-Cl bond length is in the order



When the ligand  $L = \text{CO}$ , The Cr-CO bond length is equal to 1.853 Å, which is nearly similar to Cr-CO bond length when the CB is replaced by pip as was shown in Table 5.3. The trans Cr-CO bond length is shorter in both compounds  $\text{Cr}(\text{CO})_5\text{CB}$  and  $\text{Cr}(\text{CO})_5\text{pip}$  than in  $\text{Cr}(\text{CO})_6$ . This result can be explained as follow: Since both CB and pip are an electron donor, they donate electrons to the metal. The metal is electron rich, and to compensate for this, the metal donates electrons to the trans CO as back bonding. The bond length of the other Cr-CO in the  $\text{trans}-(\text{CB})(\text{L})\text{Cr}(\text{CO})_4$  complexes are much less affected in comparison with  $\text{Cr}(\text{CO})_6$ , which

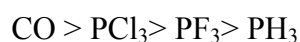
indicate that the primary effect is on the trans ligand in octahedral complexes. From Table 5.8 different ligands have different electronic properties, which cause them to bond differently to the metal center. The bond length between the Cr and CB is longer when L = CO. This is in a good agreement with which is known experimentally [10]. An explanation of this phenomenon is presented below: In the ligands used in this study, the  $\pi$  back-bonding and  $\sigma$ -donating ability are shown below [41, 55]:



Also, it's well known that  $\text{PF}_3$  is a better  $\pi$  accepting than  $\text{PH}_3$ . The text book explanation is that electronegative substituent lower the energy of the d orbitals on phosphorus and therefore make them more available for bonding [52]. The electronic effect of a ligand is most likely caused by its  $\sigma$ -donating and its  $\pi$  back-bonding abilities [10]. The better donor ligands will stabilize the transition state [10] and therefore increase the rate of dissociation of CB. The better  $\pi$ -acceptor ligands will make the metal more acidic [10]. This reduces the bonding between the metal and CB, and increases the rate of CB dissociation. It is clear from this discussion that, the electronic effect on the rate of CB dissociation is due to both  $\sigma$ -donating and  $\pi$  back-bonding abilities of the ligand bonded to the metal. The CO is well known as a good  $\pi$ -acceptor ligands but its  $\sigma$ -donating ability is unclear [10]. For example, Graham [45] determined CO to be a better  $\sigma$ -donor than  $\text{PF}_3$ . However, Hall disagrees with Graham's results,

and he concluded that CO's act as electron reservoirs [10]. In other words, the CO's will donate electrons whenever the metal needs them. This may cause a stabilization of the transition state and increase the rate of CB dissociation.

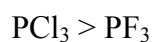
In our study, the trend of the ligands according to their back-bonding is



This trend is in agreement with the given experimental data. Taylor described a series of ligands according to their ability of  $\pi$ -acceptor. Some of these ligands are [10]:



Our results have disagreement with Taylor trend where the ligand ability of  $\pi$  acceptor trend in our calculation is



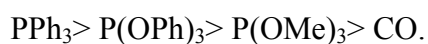
Experimentally, the rate of CB dissociation when L is CO is faster than the rate of CB dissociation when L is  $\text{PR}_3$  [10], where R is phosphine. The effect of L on the dissociation of  $\text{PPh}_3$  from  $\text{trans}-(\text{L})(\text{PPh}_3)\text{Cr}(\text{CO})_4$ , Crystal structure as shown in Table 5.9 showed that the Cr- $\text{PPh}_3$  bond length increases as the  $\pi$ -accepting ability of the trans ligand increases, which is in a good agreement with the results presented in the present study for Cr-CB bond lengths of  $\text{trans}-(\text{CB})(\text{L})\text{Cr}(\text{CO})_4$ .

**Table 5.9** The Cr-PPh<sub>3</sub> bond lengths of trans-Cr(CO)<sub>4</sub>(L)(PPh<sub>3</sub>)

L	Cr-PPh <sub>3</sub>
Pbu <sub>3</sub>	2.345
P(OMe) <sub>3</sub>	2.362
P(OPh) <sub>3</sub>	2.393
CO	2.422

Ref [10]

In a similar study, Atwood [10] examined the ligand dissociation of L from trans-(L)(PPh<sub>3</sub>)Cr(CO)<sub>4</sub>. He concluded that the rate of trans PPh<sub>3</sub> displacement increases as the size of L increases, where the order of PPh<sub>3</sub> dissociation as a function of L is



This order is opposite to the well known trans effect and to our calculated results in our study. The dominant effect in the trans ligand is the electronic properties of the trans ligand. It is inconceivable to envision a steric effect from a trans position.

### 5.6 Predicted Energy of trans-(CB)(L)Cr(CO)<sub>4</sub> Complexes, where L = CO, PH<sub>3</sub>, PCl<sub>3</sub> and PF<sub>3</sub>

Energy of the system is one of important quantities which can be predicted by Gaussian calculations. It is located approximately three

screens back from the end of the output file. For example, The total energy of the trans-(chlorobenzene)(PCl<sub>3</sub>)Cr(CO)<sub>4</sub> system, computed at Hartree-Fock level, is given by this line of the output:

SCF Done: E(RHF) = -3903.17455117 a.u. after 1 cycles

The value is in Hartrees. One Hartree is 627.51 kcal-mol<sup>-1</sup>. The number of cycles it took the SCF calculation to converge is also given on this line. The energy of trans-(CB)(L)Cr(CO)<sub>4</sub> Complexes, where L = CO, PH<sub>3</sub>, PCl<sub>3</sub> and PF<sub>3</sub> were calculated using DFT level of theory with 6-311G(D) basis set. The predicted energies are in Table 5.10.

**Table 5.10** Predicted energies of trans-(CB)(L)Cr(CO)<sub>4</sub> complexes, where L = CO, PCl<sub>3</sub>, PF<sub>3</sub>, PH<sub>3</sub>

L trans to CB	Energy (Hartree)
CO	-2303
PCl <sub>3</sub>	-3914
PF <sub>3</sub>	-2831
PH <sub>3</sub>	-2533

### 5.7 Predicted Vibration Frequencies of trans-(CB)(L)Cr(CO)<sub>4</sub> Complexes, where L = CO, PH<sub>3</sub>, PCl<sub>3</sub> and PF<sub>3</sub>

The vibration frequencies of trans-(CB)(L)Cr(CO)<sub>4</sub> complexes, where L = CO, PCl<sub>3</sub> and PF<sub>3</sub>, PH<sub>3</sub> were computed by the B3LYP level of theory

combined with 6-311G(D), and LanL2dZ basis sets as the ones used for geometry optimization. The predicted unscaled data are shown in the Table 5.11 where L= CO, PCl<sub>3</sub> and PF<sub>3</sub>, PH<sub>3</sub> respectively. All the calculated frequencies were factorized by 0.956 for the comparison with the experimental value of free CO:  $\nu(\text{CO})_{\text{exp}} = 2143 \text{ cm}^{-1}$  [49], and the calculated one is  $\nu(\text{CO})_{\text{B3LYP}} = 2211 \text{ cm}^{-1}$ . The scaled frequencies are listed in Table 5.12. All the calculations were carried out using the Gaussian 98 program. The computed frequencies of CO in the trans-(CB)(L)Cr(CO)<sub>4</sub> where L = CO are 2044 cm<sup>-1</sup>, 2045 cm<sup>-1</sup>, 2070 cm<sup>-1</sup>, and 2029 cm<sup>-1</sup>, after scaling with the scale factor 0.956, these values become 1954 cm<sup>-1</sup>, 1955 cm<sup>-1</sup>, 1981 cm<sup>-1</sup>, 1939 cm<sup>-1</sup>, respectively.

**Table 5.11** The predicted unscaled carbonyl frequencies of trans-(CB)(L)Cr(CO)<sub>4</sub> where L = CO, PCl<sub>3</sub> and PF<sub>3</sub>, PH<sub>3</sub>, respectively

L	Vibration Frequencies (IR intensity)
CO	2044 (1762), 2045 (1895), 2070 (69), 2029 (984)
PCl <sub>3</sub>	2053 (1447), 2055 (1623), 2082 (497)
PF <sub>3</sub>	2045 (1624), 2048 (1811), 2075 (148)
PH <sub>3</sub>	2007 (1850), 2006 (1855), 2039 (63)

Each one of the scaled frequencies is lower than the free CO frequency.

This result is due to the  $\pi$ -back donation from the metal to the (CO) s.

The trans CO and also the other (CO)s in trans-(CB)(L)Cr(CO)<sub>4</sub> benefit from increased back-bonding to give shorter and stronger Cr-CO. This reduces the frequency of C-O, causing a reduction in the C-O bond order which can be seen in the optimized structure of trans-(CB)(L)Cr(CO)<sub>4</sub>. (See Figure 5.9).

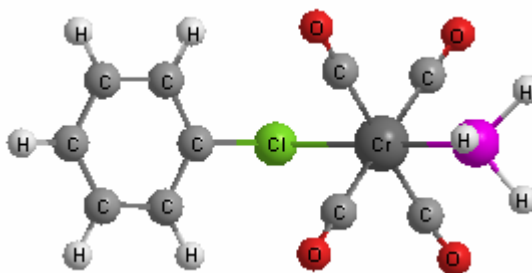


**Figure 5.9** Optimized structure of trans-(CB)(PH<sub>3</sub>)Cr(CO)<sub>4</sub>

The CO bond length equals 1.15 Å in trans-(CB)(L)Cr(CO)<sub>4</sub> which is longer than the free CO bond length which is equals 1.128 Å [49]. Note that the trans Cr-CO bond is shorter than the cis Cr-CO bond. This is because the CB group is a sigma donor, so the trans carbonyl ligand benefits from increased back-bonding to give shorter and stronger Cr-CO. Each carbonyl frequency of the metal compounds trans-(CB)(L)Cr(CO)<sub>4</sub>, where L = CO, PH<sub>3</sub>, PCl<sub>3</sub>, and PF<sub>3</sub> which are listed in Table 5.13 is lower than the frequency of the free CO. This is the case because each of ligands L = CO, PH<sub>3</sub>, PCl<sub>3</sub> and PF<sub>3</sub> has the ability of  $\pi$ -back bonding.

The convenient trends that are observed in the IR spectra of carbonyl complexes are consistent with the concept of  $\pi$ -back-bonding discussed above: The better the sigma-donating capability of the other ligands on the metal, the lower the CO stretching frequency.

**Table 5.12** Unscaled vs. scaled metal carbonyls frequencies of trans-(CB)(L)Cr(CO)<sub>4</sub> where L = CO, PCl<sub>3</sub>, PF<sub>3</sub>, PH<sub>3</sub>

L	Cr-CB Å	CO Å	$\nu$ (CO)cm <sup>-1</sup>	Scaled frequency
CO	2.658	1.144	2044 <i>E</i> , 2045 <i>E</i>	1954, 1955
			2070 <i>A</i> <sub>1</sub> , 2029 <i>A</i> <sub>1</sub>	1979 <i>A</i> <sub>1</sub> , 1940 <i>A</i> <sub>1</sub>
PCl <sub>3</sub>	2.642	1.143	2053 <i>E</i> , 2055 <i>E</i> , 2082 <i>A</i> <sub>1</sub>	1963 <i>E</i> , 1965 <i>E</i> , 1990 <i>A</i> <sub>1</sub>
PF <sub>3</sub>	2.633	1.144	2045 <i>E</i> , 2048 <i>E</i>	1955 <i>E</i> , 1958 <i>E</i> ,
			2075 <i>A</i> <sub>1</sub>	1984 <i>A</i> <sub>1</sub>
PH <sub>3</sub>	2.619	1.150	2006 <i>E</i> , 2007 <i>E</i> ,	1918 <i>E</i> , 1919 <i>E</i>
			2039	1949 <i>A</i> <sub>1</sub>
Free CO		1.128 <sup>a</sup>		2143 <sup>a</sup>

<sup>a</sup>[49]

### 5.8 Potential Energy Surface Scans

With Gaussian 98, one can perform a potential energy surface scan; thereby one can explore a region of a potential energy surface. This calculation performs a series of single point energy calculations at various structures, thereby sampling points on the potential energy surface. To request a scan job, the **Scan** keyword must be included in the route section. The variables in the molecular structure which are to vary and the range of values which they should take on must be specified. When only

one variable is allowed to vary, the scan begins at the structure where the specified variable is equal to initial-value. At each subsequent point, increment-size is added to the current value for the variable. The process is repeated until a number of single point energies have been completed. The result of a potential energy surface scan appears following this heading within the Gaussian output: **Summary of the potential surface scan**

### **5.8.1 Potential Energy Surface Scans of trans-(CB)(PCl<sub>3</sub>)Cr(CO)<sub>4</sub>**

A potential energy surface scan has been performed on the trans-(CB)(PCl<sub>3</sub>)Cr(CO)<sub>4</sub>. Our purpose here is to find the Cr-CB bond energy. The minimum energy structure of this structure is at 2.65 Å Cr-CB bond lengths as shown in Figure 5.10. Through this scan we anticipated to calculate the bond energy Cr-CB, however, the program crashes, so we resorted to the calculations as in section 5.9.

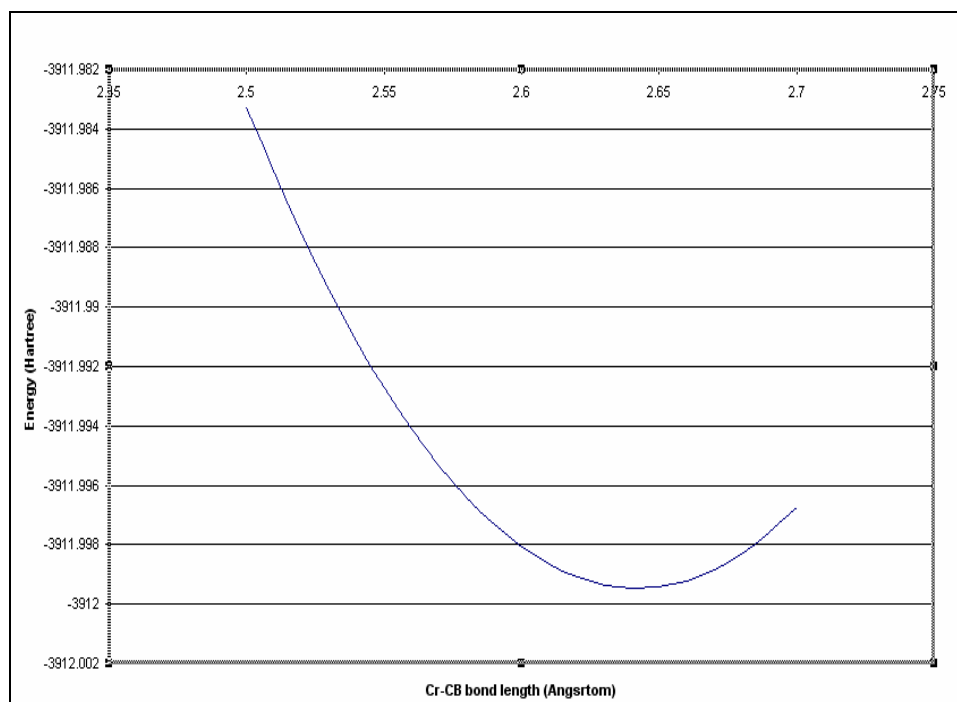


**Figure 5.10** Plot of the energies of  $\text{trans-(CB)(PCl}_3\text{)Cr(CO)}_4$  at each point of the Cr-CB bond distance at DFT level of theory using 6-311G(D) basis set

## 5.9 The Binding Energy

Accurate estimates of the breaking and forming of M-ligand bond energies in organometallic chemistry are essential for the understanding of many processes, ranging from organometallic synthesis to catalysis, surface chemistry, photo physics, and photochemistry [56]. Unfortunately, the first bond dissociation energies of a carbonyl ligand are hard to determine experimentally [56]. Thus, accurate theoretical data for the energetics of M-CO bond are needed to compensate for the scarce experimental data. Density functional theory (DFT) has proven to be a

powerful tool in predicting geometrical and thermodynamic properties of Organometallic complexes [55].

### 5.9.1 Overall Stability

The main parameter used to judge the overall stability of a complex is the binding energy listed in Table 5.13, which is defined as [53]

$$B.E = E[trans - (CB)(L)Cr(CO)_4] - [E((CB)Cr(CO)_4) + E(L)] \quad (5.2)$$

The geometries of the fragments are calculated using single point energy calculation. The level of the theory used in this calculation is DFT with 6-311G(D) basis sets. These fragments are extracted from the corresponding optimized structures. The energy is transformed from Hartree to Kcal/mol. One Hartree is 627.51 kcal/mol = 2626KJ/mol. We present here the B.E obtained using B3LYP with 6-311G(D). The trans-Cr(CO)<sub>5</sub>-(CB) complex has a B.E of 9.72 kcal/mol, followed by trans-(PCl<sub>3</sub>)Cr(CO)<sub>4</sub>-(CB) ( 10.64 kcal/mol), followed by trans-(PF<sub>3</sub>)Cr(CO)<sub>4</sub>-(CB) ( 10.92 kcal/mol), and trans-(PH<sub>3</sub>)Cr(CO)<sub>4</sub>-(CB) ( 10.96 kcal/mol), With trans-(PH<sub>3</sub>)Cr(CO)<sub>4</sub>-(CB) having the highest B.E of 10.96 kcal/mol. It is thus seen that this complex is the most stable.

The observed trend in the bond energy is in total agreements with the bond distances obtained which are listed in Table 5.8, where shorter bond means stronger bond. The binding energy when L is PH<sub>3</sub> =10.9626 kcal/mol which is greater than the binding energy when L is PF<sub>3</sub> equals

10.9190 kcal/mol, which indicates that the bond strength between CB and Cr is stronger when L is PH<sub>3</sub> than when L is PF<sub>3</sub>. This is in agreement with our calculation of the bond length as shown in Table 5.8 and in agreement with the fact that PF<sub>3</sub> has more  $\pi$  accepting ability than PH<sub>3</sub> [52].

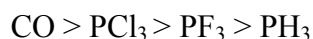
**Table 5.13** Binding energy of Cr-CB of trans-(CB)(L)Cr(CO)<sub>4</sub>, where L = CO, PCl<sub>3</sub>, PF<sub>3</sub>, PH<sub>3</sub>

L	Trans- (Cr)(L)Cr(CO) <sub>4</sub>	Cr(CO) <sub>4</sub> L	CB	CB+ Cr(CO) <sub>4</sub> L	B.E <sup>a</sup> Kcal/mol
CO	-2303.27	-1611.33	-692	-2303.30	9.72
PCl <sub>3</sub>	-3912.00	-3220.06	-692	-3912.00	10.64
PF <sub>3</sub>	-2831.00	-2139.04	-692	-2831.00	10.91
PH <sub>3</sub>	-2533.10	-1841.12	-692	-2833.00	10.96

$$^a B.E = E[\text{trans} - (\text{CB})(\text{L})\text{Cr}(\text{CO})_4] - [E((\text{CB})\text{Cr}(\text{CO})_4) + E(\text{L})]$$

## Conclusion

The electronic structures and vibration frequencies of  $\text{Cr}(\text{CO})_6$ ,  $\text{Cr}(\text{CO})_5\text{pip}$ ,  $\text{Cr}(\text{CO})_5\text{CB}$  complexes have been studied by high ab-initio HF and density functional theory using various basis sets. For the  $\text{Cr}(\text{CO})_6$ ,  $\text{Cr}(\text{CO})_5\text{pip}$ , and  $\text{Cr}(\text{CO})_5\text{CB}$  complexes, the density functional theory with 6-311G(d) gave results for the structure and vibration frequencies of such compounds which are in agreement with the experimental data. The discrepancy between the experimental and the theoretical values is due to the limitations in the one particle basis. The same calculations have been performed on a series of chromium carbonyl complexes, of the type  $\text{trans}-(\text{CB})(\text{L})\text{Cr}(\text{CO})_4$ , where  $\text{L} = \text{CO}$ ,  $\text{PH}_3$ ,  $\text{PCl}_3$  and  $\text{PF}_3$  to explore the effect of these ligands on the Cr-Cl bond. The influence of these ligands on the properties of these complexes was compared with the behavior of the carbonyl complex  $\text{Cr}(\text{CO})_6$ . Most obvious effect observed on the Cr-Cl bond was when  $\text{L} = \text{CO}$ . The ligands can be placed in the following order according to their influence on the Cr-(CB) bond



This arrangement is consistent with the  $\pi$  back-bonding capacity of the trans ligand to CB. This effect in the octahedral complexes is similar to the trans effect in square planar complexes. It is most likely that the trans influence is a ground state effect; that is, the better  $\pi$ -accepting ligand reduces the bonding between CB and the metal center. As the  $\pi$  accepting

ability of L increases, the electron density between L and the metal center increases. As the electron density between L and the metal center increases, the electron density between the metal center and CB decreases. This weakens the bond between CB and the metal. This indicates that the size of the ligands is not important in the  $\text{trans-(CB)(L)Cr(CO)}_4$  complexes. The calculated IR frequencies in these complexes are in good agreement with the known reported experimental IR frequencies. The calculated bond energy for Cr-CB is in agreement with the calculated bond distance of Cr-CB, where the shorter bond is a stronger bond.

## References

- [1] Torsti, T. **2003**. *Real-space electronic structure calculations for nanoscale*. PhD Thesis, Univ. of Helsinki : Laboratory of Physics.
- [2] Dorsett, H.E. **2000**. Overview of Molecular Modeling and ab-initio Molecular Orbital Methods Suitable for Use with Energetic Materials. DSTO Technical report.
- [3] Heiskanen, M.T., Torsti, T., Puska, M.J., Nieminen, R.M. **2001**. Multigrid method for electronic structure calculations. *J. Am. Chem. Soc.*, 63, 245106
- [4] Foresman, J.B., Frisch, C. **1996**. *Exploring Chemistry with Electronic Structure Methods*, 2<sup>nd</sup> ed., Gaussian Inc., Pittsburgh, PA.
- [5] Young, D.C. **2001**. *Computational Chemistry: A practical Guide for Applying Techniques to Real-World Problems*. New York: John Wiley & Sons, Inc.
- [6] Bytheway, I., Wah Wong, M. **1998**. The prediction of vibrational frequencies of inorganic molecules using density functional theory. *Chem. Phys. Lett*, 282: 219-226.
- [7] Barnes, L.A., Liu, B.R., Lindh, R. **1993**. Structure and energetics of Cr(CO)<sub>6</sub> and Cr(CO)<sub>5</sub>. *J. chem. phys*, 98(5): 3978-3989.
- [8] Graham, T.W. **1992**. *Organic Chemistry*, 5<sup>ed</sup>. New York: John Wiley & Sons, Inc.
- [9] Asali, K.J., Smith, J.P., Ladogana, S., Dobson, G.R. **1998**. Fast non-dissociative cis-to-trans isomerization in the cis-(P(O-i-Pr)<sub>3</sub>)<sub>2</sub>Cr(CO)<sub>4</sub> intermediate. *Inorg. chem. Commu*, 87-89.

[10] Awad, H. **1989**. *Thermal and flash photolysis studies of ligand-exchange reactions of substituted metal carbonyl complexes of Cr and Mo*. PhD Thesis, Univ. of Denton Texas.

[11] Ladogana, S., Nayak, S.K., Smit, J.p., Dobson, G.R. **1998**. The kinetics and mechanism of ligand exchange in photogenerated ( $\eta^1$ -bromobenzene)Cr(CO)<sub>5</sub>/alkene systems. *Inorg Chim Acta*, 267: 49-54.

[12] Ladogana, S., Dobson, G.R. **1998**. Bonding modes of arenes in photogenerated (arene) Cr(CO)<sub>5</sub> Complexes. *Inorg. Chem. Acta*, 271: 105-111.

[13] Kollmar, C. **1998**. Simplified Approach to the Density Functional Theory of Molecules. *Z. Naturforsch*, 54: 101–109

[14] Rauk, A. **2001**. *Orbital Interaction Theory of Organic Chemistry*, Second Edition. John Wiley & Sons, Inc.

[15] McQuarrie, D.A., Simon. J.D. **1997**. *Physical Chemistry A Molecular Approach*. California: Sausalito.

[16] Kirkby, S. 2002. *Introduction to Quantum Chemistry*

[17] Murrell, J.N., Kettle, S.F., Tedder, J.M. **1985**. *The chemical bond*. New York: John Wilet & Sons, Inc.

[18] Alberty, R.A., Silbey, R.j. **1992**. *Physical Chemistry*. New York, John Wiley & Sons, Inc.

[18] chen, Y. **2000**. *Quantum chemical Studies of Iron Carbonyl Complexes-Structure and Properties of  $(CO)_4FeL$ Complexes*. PhD thesis, Univ of Marburg.

[19] Richard, P. **1999**. *Techniques and Applications of Quantum Monte Carlo*. . PhD Thesis, Univ. of Cambridge.

[20] Sherrill, C.D. **1997**. *A Brief Review of Elementary Quantum Chemistry*. School of Chemistry and Biochemistry, Georgia Institute of Technology.

[21] Labanowski, J. K. Simplified introduction to AB initio basis set. Terms and notation. Ohio Supercomputer Center:1224 kinear Rd.

[22] Salter-Duke, B. **1998**. Basis sets – General Introduction. Northern Territory University  
<http://www.smps.ntu.edu.au/msc/>

[23] The shodor education foundation, Inc, "Background Reading for Basis Sets".  
<http://www.shodor.org/chemviz/basis/teachers/background.html>

[24] Frisch, A. and Frisch, M.J. **1998**. Gaussian 98 User's Reference, Gaussian Inc., Pittsburgh, PA.

[25] Jansen, A.P.J. **2003**. *The Chemical Bond*. Endhoven: Schuit instiute of catalysis.

[26] David, C. **2000**. An Introduction to Hartree-Fock Molecular Orbital Theory. Georgia Institute of Technology: School of Chemistry and Biochemistry

[27] McCarthy, S. **2000**. *Calculation of the Electronic Structure of N Electron Quantum Dots using the Hartree-Fock Method*. Bachelor Thesis, Univ. of Western Australia.

[28] Roudgar, A. **1999**. *Ab-initio electronic structure calculations with quantum protons*. . PhD Thesis, Univ. of ICTP

[29] Basics of Density Functional Theory:

<http://www.physics.ohio-state.edu/~aulbur/bdft/bdft1.html>

Edited by: [aulbur@mps.ohio-state.edu](mailto:aulbur@mps.ohio-state.edu)

[30] The Nobel Prize in Chemistry **1998**

(URL: <http://www.nobel.se/chemistry/laureates/1998/index.html>)

[31] Rosch, N. **1996**. *Density Functional Theory in Quantum Chemistry: Application of the Parallel Program ParaGauss*. Fachgebiet Theoretische Chemie, Techn. Universitat

[32] Kurth, S.M., Marques, M.A.L., Gross, E.K.U., **2003**. *Electronic Structure: Density Functional Theory*. Institut fur Theoretische Physik, Freie Universit"at Berlin, Arnimallee 14, D-14195 Berlin, Germany.1-8

[33] Wysokinska, R., Michalska, D. **2001** .The performance of different density functional methods in the calculation of molecular structures and vibrational spectra of platinum(II) antitumor drugs: Cisplatin and Carboplatin. *J. Comp. Chem*, 22(9): 901-912.

[34] Stratmann, R.E., Burant, J.C., Scuseria, G.E. **1997**. Improving harmonic vibrational frequencies calculations in density functional theory. *J. chem. phys*, 106(24): 10175-10183.

[35] Magyar, R.J. **2004**. Density-functional theory in one dimension for contact-interacting fermions. *Phys. Rev*, 70, 032508

[36] Cohen, R.D., Sharil, D. **2001**. The performance of density functional theory for equilibrium molecular properties of symmetry breaking molecules. *J. Chem. phys*, 114(19): 8257-8269.

[37] Perdew, J.P. Kurth. Density Functionals for Non-Relativistic Coulomb Systems. Tulane University, New Orleans, LA 70118, USA.

[38] Janoschek, R. 2001. Quantum Chemical B3LYP/cc-pvqz Computation of Ground-State Structures and Properties of Small Molecules with Atomz (HYDROGEN TO ARGON). *Pure Appl. Chem*, 73(9): 1521–1553.

[39] Ivonov, S., Burke, K., Levy, M. **1999**. Exact high-density limit of correlation potential for two-electron density. *J. Chem.Phys*, 110(21): 10262-10268.

[40] Johnson, B.G., Fisch, M.J. **1994**. An implementation of analytic second derivatives of the gradient-corrected density functional energy. *J.Chem.phys*, 100(10): 7429-7442.

[41] Myrta Gruning, M. **2003**. *Density functional theory with improved gradient and orbital dependent functionals*. PhD Thesis, Univ. of Vrije Universiteit Amsterdam.

[42] Chermette, H. **1998**. Density functional theory A powerful tool for theoretical studies in coordination chemistry. *coord. Chem. Rev*, 178-180: 699-721.

[43] Lam, K., Cruz, F.G., Burke, K. 1998. Virial Exchange Correlation Energy Density in Hooke's Atom. *J. Quan. Chem*, 69. 4: 534-540.

[44] Hieringer, W., Herrmann, W.A. 1999 Quantum chemical calculations on catalytically active transition metal complexes. *Garching bei M'unchen, Germany*. 85747. 169-171

[45] Towler, M.D., Causa, M. 1996. Density functional theory in periodic systems using local Gaussian basis sets. *Computer physics Communications*, 98: 181-205.

[46] Frisch, M.J., Trucks, G.W., Schlegel, H.B., Scuseria, G.E., Robb, M.A., Cheeseman, J.R., Zakrzewski, V.G., Montgomery, J.A. Jr., Stratmann, R.E., Burant, J.C., Dapprich, S., Millam, J.M., Daniels, A.D., Kudin, K.N., Strain, M.C., Farkas, O., Tomasi, J., Barone, V., Cossi, M., Cammi, R., Mennucci, B., Pomelli, C., Adamo, C., Clifford, S., Ochterski, J., Petersson, G.A., Ayala, P.Y., Cui, Q., Morokuma, K., Malick, D.K., Rabuck, A.D., Raghavachari, K., Foresman, J.B., Cioslowski, J., Ortiz, J.V., Stefanov, B.B., Liu, G., Liashenko, A., Piskorz, P., Komaromi, I., Gomperts, R., Martin, R.L., Fox, D.J., Keith, T., Al-Laham, M.A., Peng, C.Y., Nanayakkara, A., Gonzalez, C., Challacombe, M., Gill, P.M.W., Johnson, B., Chen, W., Wong, M.W., Andres, J.L., Gonzalez, C., Head-Gordon, M., Replogle, E.S., and Pople, J.A. (1998) Gaussian 98, Rev. A.3, Gaussian Inc., Pittsburgh PA.

[47] Chem3D 3.5 user manual, Cambridge Soft, MA (1996).

URL - <http://www.camsoft.com/>

[48] Nocedal, J., Wright, S.J. 1999. *Numerical Optimization*. Springer-Verlage New York, Inc.

[49] Mogi, K., Sakai, Y., Sonoda, T., Xu, Q., Souma, Y. **2001**. Geometry and electronic structure of binuclear metal carbonyl cations,  $[M_2(CO)_2]_{2+}$  and  $[M_2(CO)_6]^{2+}$  (M=Ni, Pd, Pt). Elsevier, *Journal of molecular structure, Theochem*, 537: 125-138.

[50] Douglas, B., McDaniel, D., Alexander, J. **1994**. *Concepts and model of inorganic chemistry*, 3<sup>ed</sup>. New York: John Wiley & Sons, Inc.

[51] Bodner, G.M. **1975**. A Fourier Transform Carbon-13 Nuclear Magnetic Resonance Study of Group 6B Transition Metal Carbonyl Complexes *Inorg.Chem*, 14(11): 2694-2699.

[52] Marynick, D.S. **1984**.  $\pi$ -Accepting Abilities of Phosphines in Transition-Metal Complexes. *J. Am. chem. Soc*, 106: 4064-4065.

[53] Creve, S., Pierloot, K., Tho Nguyen, M., Vanquickenborne, L.G. **1999**. Phosphinidene Transition Metal Complexes: A combined AB Initio MO-DFT Study of  $Cr(CO)_5PR$ . *J. Inorg. Chem*, 107-115.

[54] Coe, B.J., Glenwright, S.J. **2002**. Trans-effects in octahedral transition metal complexes. *Coord. Chem. Rev*, 203: 5–80.

[55] Goumans, T.P.M., Ehlers, A.W., van Hemert, M.C., Rosa, A. **2003**. Photodissociation of the Phosphine-Substituted Transition Metal Carbonyl Complexes  $Cr(CO)_5L$  and  $Fe(CO)_4L$ : A Theoretical Study. *J. am.chem. soc*, 125: 3558-3567.

[56] Rosa, A., Ehlers, A.W., Baerends, E.J., Snijders, J.G., te Velde, G. **1996**. Basis set effects in density functional calculations on metal-ligand

and metal-metal bonds of  $\text{Cr}(\text{CO})_5\text{-CO}$  and  $(\text{CO})_5\text{Mn-Mn}(\text{CO})_5$ . *J. phys. chem*, 100: 5690-5696.

[57] Dennenberg, R.J., Darensbourg, D.J. **1972**. Infrared and Kinetic Studies of Group VI Metal Pentacarbonyl Amine Compounds. *J. Inorg. chem*, 11(1): 72-77.

# Chapter

## Appendices

### 7.1 Atomic Units

This system of units is chosen to avoid cluttering the quantum mechanical equations with fundamental constants. It is based upon the choice  $\hbar = m_e = e = 1$ .

The principal quantities of interest in this system are:

Unit of length: Bohr radius,  $a_0 = 5.292 \text{ \AA}$

Unit of energy, the Hartree,  $E_H = 2626 \text{ kJ mol}^{-1}$

### 7.2 Glossary

**ab initio** a calculation that may use mathematical approximations, but does not utilize any experimental chemical data either in the calculation or the original creation of the method.

**Accuracy** how close a computed value is to the experimental value?

**Approximation** a numerical estimation of a solution to a mathematical Problem.

**Atomic units** a system of units convenient for formulating theoretical derivations with a minimum number of constants in the equations.

**B3LYP** (Becke 3 term, Lee Yang, Parr) a hybrid DFT method.

**Basis set** a set of functions used to describe a wave function.

**Bohr** atomic unit of length.

**Born-Oppenheimer approximation** assumption that the motion of electrons is independent of the motion of nuclei.

**Cartesian coordinates** system for locating points in space based on three coordinates, which are usually given the symbols x, y, z or i, j, k.

**Convergence** criteria for completion of a self-consistent field calculation.

**Correlation** name for the statement that there is a higher probability of finding electrons far apart than close to one another, which is rejected by some but not all ab initio calculations

**Davidson-Fletcher-Powell (DFP)** a geometry optimization algorithm

**Density functional theory (DFT)** a computational method based on the total electron density

**Determinant** a mathematical procedure for converting a matrix into a function or number

**Diffuse functions** basis functions that describe the wave function far from the nucleus

**Electron density (charge density, number density)** number of electrons per unit volume at a point in space

**Electronic structure** the arrangement of electrons in a molecule

**Gaussian-type orbital (GTO)** mathematical function for describing the wave function of an electron in an atom

**Hamiltonian** quantum mechanical operator for energy.

**Hartree** atomic unit of energy

**Hartree-Fock (HF)** an ab initio method based on averaged electron electron interactions

**In-core integral evaluation** algorithm that stores integrals in memory

**kinetic energy** energy that a particle has due to its motion

**Perturbation theory** an approximation method based on corrections to a solution for a portion of a mathematical problem

**Potential energy** energy that a particle has due to its position, particularly because of Coulombic interactions with other particles

**Quantum mechanics** a mathematical method for predicting the behavior of fundamental particles, which is considered to be rigorously correct when applicable (where the effects of relativity are negligible)

**Self-consistent field (SCF)** procedure for solving the Hartree-Fock equations

**pip** Piperidine

**CB** chlorobenzene

**L<sub>w</sub>** weak ligand

### 7.3 What's an "operator"?

An operator is simply a symbol that tells us to perform an operation. In the expression  $3 \times a$ , the symbol " $\times$ " is an operator that tells us to multiply  $a$  by 3. Similarly, in the expression

$$\frac{d}{dx} e^{ax} = a e^{ax}$$

the  $(\frac{d}{dx})$  symbol tells us to perform the differentiation.

### 7.4 Functional

A functional takes a function and provides a number. It is usually written with the function in square brackets as

$$F[f] = a$$

For example: take a function and integrate it from  $-\infty$  to  $+\infty$ . The formula for the expectation value is the total energy functional  $E(\psi)$ . Since it takes some function  $\psi$  and returns the value of energy for this  $\psi$ .

Functionals can also have derivatives, which behave similarly to traditional derivatives for functions. The differential of the functional is defined as :

$$\delta F[f] = F[f + \delta f] - F[f] = \int \frac{\delta F}{\delta f(x)} \delta f(x) dx$$

The functional derivatives have properties similar to traditional function derivatives, e.g.:

$$\frac{\delta}{\delta f(x)}(C_1F_1 + C_2F_2) = C_1 \frac{\delta F_1}{\delta f(x)} + C_2 \frac{\delta F_2}{\delta f(x)}$$

#### 7.4 Input Structure of Some Molecules Used in This Study

**Table 7.1** Input structure of (CB)Cr(CO)<sub>6</sub> in Cartesian coordinates

(η <sup>1</sup> -chlorobenzene)Cr(CO) <sub>5</sub>			
Cr	0.687374	-0.897449	-0.694431
C	-1.208190	-0.928119	-0.694431
O	0.667863	-0.770005	-3.767890
C	0.745344	-2.737779	-0.754042
C	0.677164	-0.810189	-2.591562
C	2.584392	-0.810062	-0.694541
C	0.698063	-0.928764	1.200732
O	0.783832	-3.918352	-0.791773
O	3.760826	-0.770911	-0.692034
O	0.711308	-0.959860	2.378748
O	-2.385925	-0.958959	-0.701324
Cl	0.687374	1.777387	-0.694431
C	-0.075705	2.710473	1.829783
C	-0.522901	2.458580	0.529399
C	-1.829195	2.707725	0.095878
C	-1.001131	3.244328	2.749567
C	-2.738253	3.241597	1.031821
C	-2.326289	3.509242	2.352220
H	0.948176	2.502432	2.123735
H	-2.134227	2.497517	-0.922957
H	-0.681532	3.446439	3.767890
H	-3.760826	3.442299	0.725165
H	-3.034549	3.918352	3.067812

**Table 7.2** Input structure of trans-(CB)(PH<sub>3</sub>)Cr(CO)<sub>4</sub> in Cartesian coordinates

trans-(CB)(PH <sub>3</sub> )Cr(CO) <sub>4</sub>			
Cr	1.250806	0.000040	-0.000695
Cl	-0.792805	-0.012493	-1.638517
C	2.128342	1.304105	-1.070694
C	0.454766	1.388445	1.017903
C	2.090050	-1.377953	-1.006966
C	0.425560	-1.315012	1.089913
P	3.048224	0.010855	1.442911
C	2.322194	-0.005177	-0.732354
O	2.713063	2.091122	-1.668876
O	2.647462	-2.209217	-1.570347
O	-0.050380	-2.117915	1.761297
O	-0.005739	2.235246	1.644668
C	2.909355	-1.219037	-0.401634
C	-2.897895	1.213957	-0.400721
C	-4.119918	-1.204002	0.288813
C	-4.108450	1.209668	0.289910
C	-4.719566	0.005543	0.633234
H	3.958163	-1.077494	1.483839
H	2.841820	0.091236	2.843796
H	4.036187	1.027536	1.374890
H	2.432147	-2.152730	-0.672158
H	-2.411661	2.143319	-0.669894
H	-4.590028	-2.143771	0.557584

**Table 7.3** Input structure of trans-(CB)(PCl<sub>3</sub>)Cr(CO)<sub>4</sub> in Cartesian coordinates

trans-(CB)(PCl <sub>3</sub> )Cr(CO) <sub>4</sub>			
Cr	-0.776328	0.323393	0.039188
Cl	1.475629	1.676046	0.217563
C	-0.080817	-0.978482	1.243081
C	-1.435646	1.667288	-1.156193
C	0.072747	0.640547	-1.447225
C	-1.445754	1.326942	1.526320
P	2.619101	0.786829	-0.104371
C	2.877012	0.585718	0.080368
O	0.331139	1.757405	1.974220
O	-1.852120	2.456322	-1.870367
O	0.341391	1.215928	-2.345888
O	-1.868558	1.912865	2.411938
F	2.564125	2.366737	-0.347399
F	-3.656121	-0.824735	1.113483
F	3.695183	0.464315	-1.243814
C	3.376721	0.007697	1.231365
C	3.443228	0.384724	1.170880
C	4.487889	0.840912	1.115374
C	4.554085	0.451520	-1.266378
C	5.075875	1.062446	-0.128135
H	2.911239	0.171562	2.192421